

Thermal production of astrophobic axions

Marcin Badziak¹ Keisuke Harigaya^{2,3,4} Michał Łukowski¹ Robert Ziegler⁵

¹*Institute of Theoretical Physics, Faculty of Physics, University of Warsaw, ul. Pasteura 5, PL-02-093 Warsaw, Poland*

²*Department of Physics, University of Chicago, Chicago, IL 60637, USA*

³*Enrico Fermi Institute and Kavli Institute for Cosmological Physics, University of Chicago, Chicago, IL 60637, USA*

⁴*Kavli Institute for the Physics and Mathematics of the Universe (WPI), The University of Tokyo Institutes for Advanced Study, The University of Tokyo, Kashiwa, Chiba 277-8583, Japan*

⁵*Institut für Theoretische Teilchenphysik, Karlsruhe Institute of Technology, Karlsruhe, Germany*

ABSTRACT: Hot axions are produced in the early Universe via their interactions with Standard Model particles, contributing to dark radiation commonly parameterized as ΔN_{eff} . In standard QCD axion benchmark models, this contribution to ΔN_{eff} is negligible after taking into account astrophysical limits such as the SN1987A bound. We therefore compute the axion contribution to ΔN_{eff} in so-called astrophobic axion models characterized by strongly suppressed axion couplings to nucleons and electrons, in which astrophysical constraints are relaxed and ΔN_{eff} may be sizable. We also construct new astrophobic models in which axion couplings to photons and/or muons are suppressed as well, allowing for axion masses as large as few eV. Most astrophobic models are within the reach of CMB-S4, while some allow for ΔN_{eff} as large as the current upper bound from Planck and thus will be probed by the Simons Observatory. The majority of astrophobic axion models predicting large ΔN_{eff} is also within the reach of IAXO or even BabyIAXO.

Contents

1	Introduction	1
2	QCD Axion Couplings	3
2.1	Axion Effective Lagrangian	3
2.2	Constraints on Axion Couplings	4
2.2.1	Nucleon Couplings	4
2.2.2	Pion Couplings	5
2.2.3	Electron Coupling	5
2.2.4	Muon Coupling	5
2.2.5	Photon Coupling	6
2.2.6	Flavor-violating Couplings	6
3	Model-independent Analysis of ΔN_{eff}	6
4	ΔN_{eff} in Astrophobic 2HDMs	9
5	ΔN_{eff} in Astrophobic 3HDMs	14
5.1	Models with $ C_\mu \ll 1$	15
5.2	Models with $ C_\gamma \ll 1$	17
5.3	Models with $ C_\mu \ll 1$ and $ C_\gamma \ll 1$ and LFV	18
6	ΔN_{eff} from the Naturally Astrophobic QCD Axion	19
7	Conclusions	23
A	Axion Couplings to Pions and Kaons	25
A.1	Coupling to Pions	26
A.2	Coupling to Kaons	26
B	Axion Production Rates	27
B.1	Equilibrium Number Densities	27
B.2	Collision Operators and Production Rates	27
B.3	Pion and Kaon Scatterings	30
B.4	Lepton flavor-conserving Scatterings	30
B.5	Lepton flavor-violating Decays	32
C	Boltzmann Equation	32
C.1	Approximate Solution to Boltzmann Equation	34
C.2	Thermal Freeze-Out	36
C.3	Thermal Freeze-In	36
C.4	Transition Region	36

D Astrophobic DFSZ Models	37
D.1 Quark Yukawa Sector	37
D.2 Axion Couplings	38
D.3 Scalar Potential	40
D.4 Nucleophobic Models	40
D.5 Lepton Yukawa Sector	43

1 Introduction

Among the most compelling solutions to the strong CP problem is the Peccei-Quinn (PQ) mechanism [1, 2] that predicts the existence of a new light pseudoscalar particle called the QCD axion [3, 4], which is also an excellent candidate for cold dark matter (DM). Most of the parameter space in which the axion can explain the observed DM abundance has not been probed experimentally, but several experiments targeting the most interesting axion region are in preparation, see Ref. [5] for a review.

To successfully account for cold dark matter, QCD axions have to be produced non-thermally in the early universe [6–8]. However, QCD axions could also be thermally produced via their interactions with the Standard Model (SM) bath, and contribute to the energy density of relativistic degrees of freedom, usually parametrized as the effective number of neutrinos N_{eff} . This axion contribution, dubbed in the following ΔN_{eff} , is constrained by observations of the cosmic microwave background (CMB) and low-redshift baryon acoustic oscillations (BAO) data. The most recent (2018) analysis from the Planck collaboration provides the combined constraint $\Delta N_{\text{eff}} \leq 0.3$ at the 95% confidence level (CL) [9]. In the near future this bound may be further improved by a factor of few with the help of the Simons Observatory, down to about 0.1 [10], and eventually by the CMB-S4 experiments down to about 0.05 [11].

The axion couples to the SM particles with strength inversely proportional to the axion decay constant f_a . For sufficiently small f_a , the axion is in thermal equilibrium with the SM bath for some range of temperatures. As the temperature drops, axion interactions become suppressed, and eventually freeze out at a temperature T_d . Smaller f_a leads to later axion decoupling from the SM bath and hence larger ΔN_{eff} , since $\Delta N_{\text{eff}} \propto g_{*s}(T_d)^{-4/3}$ (assuming instantaneous decoupling), where $g_{*s}(T_d)$ is the effective number of SM entropy degrees of freedom at T_d . On the other hand, for sufficiently large f_a , the axion is never in thermal equilibrium and only produced via its interactions with the SM bath through thermal freeze-in [12]. In this case the late-time abundance is proportional to the production rates scaling as $\propto 1/f_a^2$, so that $\Delta N_{\text{eff}} \propto f_a^{-8/3}$.

Using the current constraint¹ on ΔN_{eff} , it is therefore possible to set a lower bound on f_a , which can be further improved in the near future. The lower bound on f_a obtained

¹For sufficiently small f_a the axion is no longer relativistic at the time of recombination, and its contribution to the total energy density is constrained rather by limits on warm DM, although one can still formulate this bound in terms of ΔN_{eff} [13].

from ΔN_{eff} depends on the nature of the axion interactions, and thus is model-dependent. For example, in the KSVZ model [14, 15] the current bound is $f_a \gtrsim 2 \times 10^7$ GeV and is expected to be improved up to $f_a \gtrsim 6 \times 10^7$ GeV with CMB-S4 data [16] (see also Refs. [17, 18]). However, smaller f_a also leads to more efficient axion emission in various stellar environments, and the resulting bounds are typically much stronger than those from ΔN_{eff} . In the KSVZ model, the cooling rate of neutron stars (NS) [19] and the duration of the neutrino burst from SN1987A [20] lead, independently, to a lower bound on f_a of about 4×10^8 GeV. For such large f_a , the KSVZ model predicts $\Delta N_{\text{eff}} \lesssim 0.03$ so it is difficult to probe the KSVZ axion with cosmological data in the foreseeable future. The same conclusion is valid for simple DFSZ models [21, 22], which have been studied in the context of thermal axion production in e.g. Refs. [17, 23–26].

For this reason future experimental probes of ΔN_{eff} are only sensitive to QCD axion models in which either astrophysical bounds are absent for some reason or the relevant axion couplings are suppressed. For example, in order to relax the constraints on f_a from NS cooling and SN1987A, it is necessary to suppress simultaneously the axion couplings to protons and neutrons. This may be possible if the axion couples to up- and down-quarks in such a way that the model-independent contribution to axion-nucleon couplings from the QCD anomaly is cancelled to good approximation. Also axion couplings to electrons need to be suppressed, in order to avoid stringent constraints from white dwarfs [27]. Such models, dubbed “astrophobic” axion models, have been discussed in Refs. [28–34]. The goal of the present paper is to systematically compute ΔN_{eff} in these kind of models, which allow to satisfy astrophysical constraints with rather low f_a , and assess their prospects for discovery through ΔN_{eff} by the Simons Observatory [10] and CMB-S4 [11], laboratory searches such as IAXO [35], and the James Webb Space Telescope (JWST) [36].

In common QCD axion benchmark models the dominant contribution to ΔN_{eff} comes from axion scatterings with pions ($\pi\pi \leftrightarrow \pi a$) [37]. However, this production mode is necessarily suppressed in astrophobic axion models, because the suppression of axion-nucleon couplings also leads to the suppression of axion-pion couplings. We will show, in a model-independent way, that other contributions to ΔN_{eff} can still be sizeable, even after taking into account all astrophysical constraints. We will first discuss the original astrophobic models [28], which are two-Higgs-doublet models (2HDM) that generalize common DFSZ scenarios. By allowing for flavor non-universal PQ charges, axion couplings to nucleons and electrons can be suppressed, so that in these scenarios axions are mainly produced from lepton flavor-violating (LFV) decays $\tau \rightarrow ea$, which are unavoidable in this class of models in order to suppress the axion-electron coupling. This leads to a sharp prediction for ΔN_{eff} that only depends on f_a , which is however limited by astrophysical constraints on the axion-photon coupling and axion-muon coupling.

For this reason we consider “proper” astrophobic models, in which not only axion couplings to nucleons and electrons, but also to muons and/or photons are suppressed. Examples of such models have been recently proposed in Ref. [33], in which the coupling of the axion with SM particles are controlled by the PQ charges of SM fermions and astrophobia is naturally obtained without any tuning. See Ref. [38] for earlier attempts. We also construct new “proper” astrophobic models and show that the required suppression of

couplings can be realized in generalized DFSZ models with three Higgs doublets (3HDMs), and systematically classify such models, which not only allow for axion decay constants $f_a < 10^7$ GeV compatible with all constraints, but also to suppress the axion-electron coupling without tuning (in contrast to 2HDMs).

The rest of the article is organized as follows. In Section 2 we discuss the general QCD axion effective Lagrangian and summarise laboratory and astrophysical constraints on the axion decay constant. In Section 3 we analyse dominant channels for thermal axion production in a model independent way. In Section 4 we compute the thermal axion abundance in astrophobic 2HDMs, while in Section 5 we present a similar analysis for 3HDMs. In Section 6 we discuss cosmological constraints on the naturally astrophobic axion. We conclude our work in Section 7, which is followed by several appendices, in which we present the details of the computations of axion couplings to pions and kaons in Chiral Perturbation Theory (Appendix A), thermal axion production rates (Appendix B), approximate solutions to the Boltzmann equation (Appendix C) and the explicit construction of astrophobic models (Appendix D).

2 QCD Axion Couplings

In this section we define the general effective Lagrangian and review the laboratory and astrophysical constraints on axion couplings relevant for our analysis.

2.1 Axion Effective Lagrangian

At energies much below the PQ breaking scale, the effective axion couplings to gauge fields and fermions are given by

$$\mathcal{L} = \frac{a}{f_a} \frac{\alpha_s}{8\pi} G\tilde{G} + \frac{E}{N} \frac{a}{f_a} \frac{\alpha_{\text{em}}}{8\pi} F\tilde{F} + \frac{\partial_\mu a}{2f_a} \bar{f}_i \gamma^\mu (C_{ij}^V + C_{ij}^A \gamma_5) f_j, \quad (2.1)$$

where f_a is the axion decay constant, $F\tilde{F} \equiv 1/2 \epsilon_{\mu\nu\rho\sigma} F^{\mu\nu} F^{\rho\sigma}$ with the electromagnetic (EM) field strengths $F^{\mu\nu}$ and similar for gluons, E/N is the ratio of EM and color anomaly coefficients and we use the convention $\epsilon^{0123} = -1$. For later convenience we define $C_{ij} = \sqrt{|C_{ij}^A|^2 + |C_{ij}^V|^2}$ for the flavor-violating couplings, as thermal axion production typically does not depend on the chiral structure of axion couplings.

The first term in Eq. (2.1) gives rise to the axion mass, which can be conveniently calculated in chiral perturbation theory, giving [39]

$$m_a = 0.5691(51) \text{ eV} \left(\frac{10^7 \text{ GeV}}{f_a} \right). \quad (2.2)$$

Below the scale of the QCD phase transition the relevant couplings are those to photons, nucleons, leptons and pions,

$$\mathcal{L} = C_\gamma \frac{a}{f_a} \frac{\alpha_{\text{em}}}{8\pi} F\tilde{F} + \frac{\partial_\mu a}{2f_a} C_N \bar{N} \gamma^\mu \gamma_5 N + \frac{\partial_\mu a}{2f_a} \bar{\ell}_i \gamma^\mu (C_{ij}^V + C_{ij}^A \gamma_5) \ell_j + \frac{\partial_\mu a}{f_a f_\pi} C_\pi \partial[\pi\pi\pi]_\mu, \quad (2.3)$$

where $N = n, p$ and $\partial[\pi\pi\pi]_\mu = 2\partial_\mu\pi_0\pi_+\pi_- - \pi_0\partial_\mu\pi_+\pi_- - \pi_0\pi_+\partial_\mu\pi_-$. Matching to the UV coefficients in the Lagrangian of Eq. (2.1) gives [33]

$$C_p + C_n = 0.40(4) \left(0.95(C_u + C_d) + 0.05 - \frac{1+z}{1+z+w} \right) - 2\delta, \quad (2.4)$$

$$C_p - C_n = 1.273(2) \left(C_u - C_d - \frac{1-z}{1+z+w} \right), \quad (2.5)$$

$$C_\pi = -\frac{1}{3} \left(C_u - C_d - \frac{1-z}{1+z+w} \right), \quad (2.6)$$

$$C_\gamma = 2\pi f_a g_{a\gamma\gamma} = E/N - 2.07(4), \quad (2.7)$$

where $C_q \equiv C_{qq}^A(\mu = f_a)$, $z = m_u/m_d = 0.48(2)$, $w = m_u/m_s = 0.023(1)$, and $\delta \approx \sum_{i=s,c,b,t} \delta_i C_i$. The coefficients δ_i for $i = s, c, b$ are $\mathcal{O}(10^{-2})$, arising from QCD renormalization group (RG) effects, and their exact values can be found in Ref. [33]. On the other hand, $\delta_t \sim \mathcal{O}(0.1)$ is much larger due to RG effects induced by the large top Yukawa coupling [40–43], and its exact value is sensitive to f_a and the details of the UV model. We also note that $C_\pi \propto (C_n - C_p)$, so that pion couplings are suppressed whenever couplings to nucleons are suppressed. In the above result for C_γ we quote the value 2.07(4) obtained in Ref. [33] using the results from Ref. [44], which include the effects of the strange quark within three-flavor ChPT at NLO. This value is different from the usually quoted value 1.92(4) from Ref. [45]. Nevertheless, this difference does not have important impact on our results.

2.2 Constraints on Axion Couplings

There are several constraints on axion couplings from astrophysics and laboratory searches. In the following we collect the limits on axion couplings to nucleons, pions, electrons, muons, photons and LFV couplings, which are most relevant for our analysis.

2.2.1 Nucleon Couplings

Since the axion-gluon coupling is crucial in solving the strong CP problem with the PQ mechanism, axion-nucleon couplings are generically present and mainly constrained by astrophysical observations, prominently the duration of the neutrino burst observed in SN1987A and the cooling rate of neutron stars. The constraints obtained from SN1987A [20] and neutron stars [19] are roughly comparable, but for concreteness we only use the SN1987A bound from Ref. [20], which provides a formula for the general case when the axion couples differently to neutrons and protons:

$$0.61g_{ap}^2 + g_{an}^2 + 0.53g_{an}g_{ap} < 8.26 \times 10^{-19}, \quad (2.8)$$

where $g_{ai} \equiv C_i m_i / f_a$ with $i = n, p$. For $C_n = 0$ this leads to the lower bound

$$\frac{f_a}{|C_p|} \gtrsim 8 \times 10^8 \text{ GeV}, \quad (2.9)$$

while varying C_n in the range $|C_n| \leq |C_p|$ can strengthen the above bound by at most a factor of 2. In the KSVZ model, $C_p \approx -0.47$, which implies $f_a \gtrsim 4 \times 10^8 \text{ GeV}$. As we will

see in the next section, large values of ΔN_{eff} typically require much smaller values of f_a , and thus suppressed nucleon couplings $|C_p|, |C_n| \lesssim \mathcal{O}(10^{-2})$. Indeed axion-nucleon couplings can be suppressed if there is an approximate cancellation between the axion-gluon and axion-quark contributions [28]. This happens if $C_u \approx 2/3$ and $C_d \approx 1/3$, as can be seen from Eqs. (2.4) and (2.5). We refer to axions satisfying these criteria as “nucleophobic” axions. Due to higher order corrections to the axion-nucleon couplings, the values of f_a satisfying the bounds from SN1987A and neutron stars cannot be arbitrary low, but values as small as 10^7 GeV (or even 10^6 GeV if z is very close to 0.49) may be allowed [33].

2.2.2 Pion Couplings

Suppressed couplings to nucleons imply suppressed pion couplings. The maximal pion coupling consistent with the constraints on the nucleon couplings is obtained for $C_p \approx -C_n$. Using Eqs. (2.5) and (2.6) one can relate pion couplings to nucleon couplings

$$C_\pi \approx -\frac{1}{4}(C_p - C_n) \approx \frac{1}{2}C_n. \quad (2.10)$$

Using the bound on the neutron coupling (2.9) one can derive an upper bound on the pion coupling to the astrophobic axion:

$$C_\pi \lesssim 0.5 \frac{f_a}{10^9 \text{ GeV}}. \quad (2.11)$$

As we will see below, for an axion-pion coupling satisfying the above constraint, ΔN_{eff} from axion-pion scattering is below 0.01, and thus negligible given near future sensitivities.

2.2.3 Electron Coupling

The axion-electron coupling is constrained by the observed shape of the white dwarf luminosity function, giving the 95% CL lower bound [27]

$$\frac{f_a}{|C_e|} \gtrsim 2 \times 10^9 \text{ GeV}. \quad (2.12)$$

This implies that the axion-electron coupling must also be suppressed, at least to the level $\mathcal{O}(10^{-2})$ in order to allow for sizeable contributions to ΔN_{eff} .

2.2.4 Muon Coupling

Also the axion-muon coupling is constrained by the energy-loss argument for SN1987A [46–48], which lead to the conservative lower bound [48]

$$\frac{f_a}{|C_\mu|} \gtrsim 1.2 \times 10^7 \text{ GeV}. \quad (2.13)$$

For $\mathcal{O}(1)$ couplings the limit on f_a from the axion-muon coupling is much weaker than the bounds on nucleon and electron couplings. However, in nucleophobic and electrophobic axion models, this becomes a relevant constraint and limits the maximal contribution to ΔN_{eff} from axion scatterings with muons.

2.2.5 Photon Coupling

Observations of the evolution of horizontal branch stars in globular clusters constrain the axion-photon coupling as [49]

$$\frac{f_a}{|C_\gamma|} > 1.8 \times 10^7 \text{ GeV}. \quad (2.14)$$

In order to satisfy the above bound, f_a should be above $\mathcal{O}(10^7)$ GeV, unless the axion-photon coupling is suppressed. This is indeed the case for $E/N = 2$, as noted already in Ref. [50], and f_a down to $\mathcal{O}(10^6)$ GeV is allowed. Note also that within theoretical uncertainties even $C_\gamma = 0$ is possible for $E/N = 2$.

2.2.6 Flavor-violating Couplings

Flavor-violating axion couplings are constrained by high-intensity laboratory experiments looking for missing energy in rare decays. The strongest constraint is set by the experiments searching for $\mu \rightarrow ea$ decays at TRIUMF [51] or TWIST [52], depending on the chirality structure of the axion couplings. For purely left-handed or right-handed couplings the upper bounds at 95% CL read [53]

$$\frac{f_a}{|C_{\mu e}|} \geq 5.0 \times 10^8 \text{ GeV}, \quad \text{for } C_{\mu e}^V = -C_{\mu e}^A, \quad (2.15)$$

$$\frac{f_a}{|C_{\mu e}|} \geq 2.5 \times 10^9 \text{ GeV}, \quad \text{for } C_{\mu e}^V = C_{\mu e}^A. \quad (2.16)$$

For values of f_a where ΔN_{eff} can be non-negligible, the above limits imply $|C_{\mu e}| \ll 1$.

Constraints from flavor-violating τ -decays are much weaker. The strongest constraints have been recently provided by the Belle-II [54] collaboration, which result in the following lower bounds at 95% CL

$$\frac{f_a}{|C_{\tau e}|} \gtrsim 3.6 \times 10^6 \text{ GeV}, \quad (2.17)$$

$$\frac{f_a}{|C_{\tau \mu}|} \gtrsim 4.6 \times 10^6 \text{ GeV}. \quad (2.18)$$

Rescaling the current expected bounds provided in Ref. [54] for 62.8 fb^{-1} , Belle-II with 50 ab^{-1} can be expected to probe flavor-violating τ -couplings down to

$$\frac{f_a}{|C_{\tau e}|} \gtrsim 1.6 \times 10^7 \text{ GeV}, \quad (2.19)$$

$$\frac{f_a}{|C_{\tau \mu}|} \gtrsim 1.7 \times 10^7 \text{ GeV}. \quad (2.20)$$

3 Model-independent Analysis of ΔN_{eff}

We first perform the calculation of ΔN_{eff} in nucleophobic axion models in a model independent way, allowing all lepton-axion couplings that are consistent with experimental and

astrophysical constraints². This will allow us to understand which couplings are the most relevant for thermal axion production in astrophobic models. We do not study the impact of axion-quark couplings on ΔN_{eff} in this section, as they cannot be reliably computed due to non-perturbative effects, but will discuss their potential impact in the following sections for specific models.

A crucial feature of nucleophobic models is that the axion-pion coupling is tiny, since it is proportional to $C_p - C_n$, which in turn must be strongly suppressed to avoid axion couplings to nucleons. In contrast to common axion benchmark models, where $\pi\pi \rightarrow \pi a$ scattering is the dominant source of axion thermalization, nucleophobia implies that other processes for axion production become relevant. In Fig. 1 we show the predicted value of ΔN_{eff} as a function of f_a/C_i , assuming the presence of a single axion coupling C_i at a time. Details of the calculation are outlined in Appendices B and C.³ We restrict to leptonic couplings $C_\tau, C_\mu, C_e, C_{\mu e}, C_{\tau e}$ ($C_{\tau\mu}$ gives predictions essentially identical to $C_{\tau e}$), and also include C_π for comparison. The constraints on f_a/C_i discussed in Section 2 are taken into account by dashing the predicted curve ΔN_{eff} for values of f_a/C_i below the respective limit, while drawing it solid where the bound is respected.

Present CMB and BAO data exclude certain regions in the $(m_a, \Delta N_{\text{eff}})$ plane [13], which one can convert to limits in the $(f_a/C_i, \Delta N_{\text{eff}})$ plane using the QCD axion mass relation and fixing C_i . We show in red the region excluded for $C_i = 1$, and show the contours of the excluded regions for $C_i = 1/3$ and $C_i = 1/10$. While the bounds on the axion couplings are essentially independent of C_i for large f_a , they drastically strengthen for $f_a < \mathcal{O}(10^7)$ GeV, corresponding to $m_a > \mathcal{O}(0.6)$ eV, where the axion can no longer be treated as massless and becomes non-relativistic around recombination. Such axions affect the CMB in a different way than extra relativistic degrees of freedom. In Fig. 1 we take this into account by using the bounds on ΔN_{eff} presented in Ref. [13], which have been obtained for general axion masses.⁴ Similar effects will be relevant for the expected limits from the Simons Observatory and CMB-S4. However, in order to show the sensitivity of future experiments in Fig. 1, we conservatively assume forecasted sensitivities to ΔN_{eff} for massless axions $\Delta N_{\text{eff}}^{\text{Simons}}(2\sigma) = 0.1$ [10] and $\Delta N_{\text{eff}}^{\text{CMB-S4}}(2\sigma) = 0.054$ [11].

It is clear from Fig. 1 that for generic (flavor-universal) models, where all axion couplings are of similar size, $\pi\pi \rightarrow \pi a$ scattering gives by far the largest contribution to ΔN_{eff} . In hadronic axion models, such as KSVZ with $C_\pi \approx 0.1$, this results in the so-called hot dark matter bound $f_a \gtrsim 2 \times 10^7$ GeV, which is expected to be improved up to $f_a \gtrsim 6 \times 10^7$ GeV by CMB-S4 experiments [16]. However, the astrophysical constraints require $f_a/C_\pi \gtrsim 2 \times 10^9$ GeV (the entire C_π curve is dashed), which implies that for values

²Model-independent analyses of thermal axion production in various channels without taking into account astrophysical constraints were presented in Refs. [55–57].

³For freeze-in production, where the axion does not reach thermal equilibrium, our computation underestimates ΔN_{eff} . The underestimation is most significant for muon scattering, where it is off by at most a factor 2 in the phenomenologically relevant parameter range. The sensitivity of future CMB observations on f_a is largely unaffected by this, due to the strong dependence of ΔN_{eff} on f_a for the freeze-in case. See Appendix C for details.

⁴Note that for sufficiently heavy axions ΔN_{eff} no longer denotes extra relativistic degrees of freedom, but remains a useful parametrization of the total energy density of thermally produced axions.

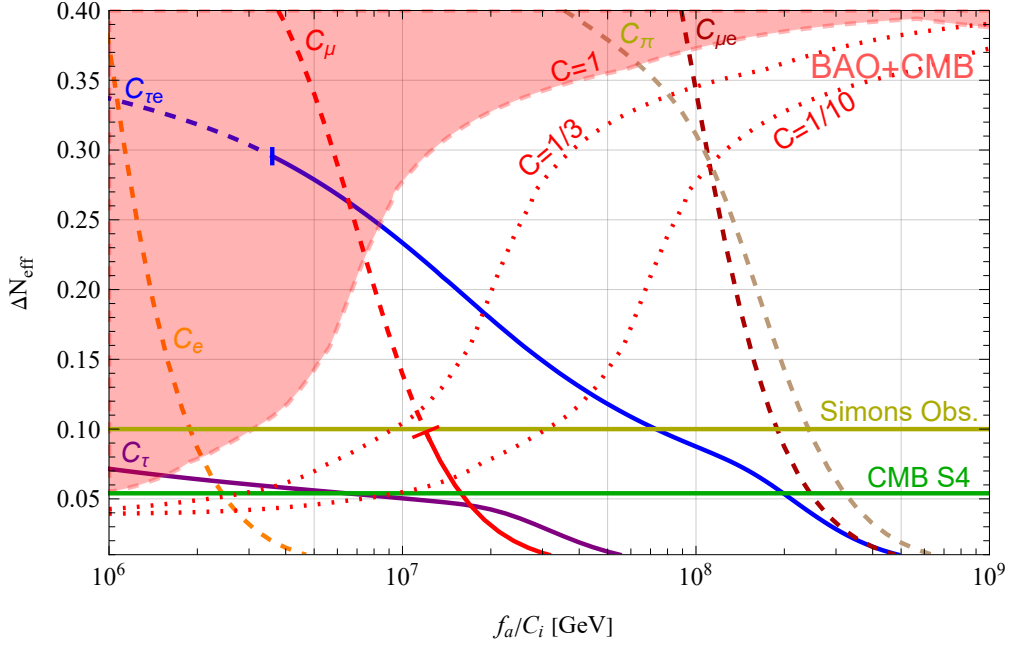


Figure 1. Additional effective number of neutrinos ΔN_{eff} as a function of f_a/C_i , for $i = \pi, \tau, \mu, e, \mu e, \tau e$. $C_{\tau\mu}$ gives predictions essentially identical to $C_{\tau e}$. The red region is excluded by BAO+CMB [13] assuming $C_i = 1$, while dotted curves show the bound for the representative values $C_i = 1/3$ and $C_i = 1/10$. Dashed (solid) lines indicate ranges of excluded (viable) values of f_a/C_i for a given type of coupling, as discussed in Section 2.2.

of f_a consistent with these constraints ΔN_{eff} is much below 0.01. Therefore axion interactions with leptons often lead to larger ΔN_{eff} than production from pion scattering, after taking into account the astrophysical constraints on f_a .

We first consider the case in which flavor-violating axion couplings are absent. Axion scatterings with electrons give non-negligible contribution to ΔN_{eff} only for f_a/C_e below $\text{few} \times 10^6$ GeV (because the scattering cross-section is suppressed by the small electron mass, cf. Appendix B), but such small values of f_a/C_e are already excluded by astrophysical constraints. The contribution to ΔN_{eff} from axion-muon scatterings is less limited by astrophysics, but after taking into account the bound from SN1987A, ΔN_{eff} from axion production off muons is at most about 0.1, which is at the verge of the future sensitivity of the Simons Observatory. Axion-tau couplings instead are not constrained by astrophysics, but axion production off taus leads to $\Delta N_{\text{eff}} > 0.05$ only for $f_a/C_\tau \lesssim 10^7$ GeV. Note that for large f_a the curves indeed follow the expected scaling $\Delta N_{\text{eff}} \propto (m_\ell/f_a^2)^{-4/3}$, cf. Appendix C.3, in particular roughly the same $\Delta N_{\text{eff}} \approx 0.01$ is obtained for constant values of m_ℓ/f_a^2 for all three leptons.

Turning to lepton flavor-violating axion couplings, it is instead possible to produce sizable values of ΔN_{eff} even for large f_a/C_i , as can be seen from Fig. 1. If all LFV couplings are of similar size, the largest contribution comes from $\mu \rightarrow ea$ axion production controlled by $C_{\mu e}$, but the strong laboratory constraints on these decays limit the resulting

contribution to ΔN_{eff} to negligible values. Instead LFV decays $\tau \rightarrow \ell a$ with $\ell = \mu, e$ that are controlled by $C_{\tau\ell}$ are much less constrained by experiments and can give sizable contributions to ΔN_{eff} . If such couplings are present, CMB-S4 will be sensitive to values of $f_a/C_{\tau\ell}$ as large as 2×10^8 GeV, which is an order magnitude stronger than the forecasted sensitivity of Belle-II, cf. Eq. (2.19). The current lower bound on f_a from ΔN_{eff} is about 8×10^6 GeV for $C_{\tau\ell} = 1$, but it is very sensitive to the actual value of $C_{\tau\ell}$, as in this regime the axion ceases to be a relativistic particle at recombination. Accordingly the bound on ΔN_{eff} gets stronger for $f_a < \mathcal{O}(10^7)$ GeV, and values of f_a much below 10^7 GeV are excluded, even for $C_{\tau\ell}$ significantly below unity. Also axion production from decays roughly follow the expected scaling for large f_a , $\Delta N_{\text{eff}} \propto (m_\ell/f_a^2)^{-4/3}$, cf. Appendix C.3.

To summarize, Fig. 1 demonstrates that sizable contributions to ΔN_{eff} from axion production in the reach of near-future experiments are possible in models where *i*) flavor-violating axion-tau couplings are sizable and *ii*) axion couplings to nucleons and electrons, as well as all other flavor-violating axion couplings, are sufficiently suppressed in order to allow for $f_a \lesssim 10^8$ GeV. The above requirements can be fulfilled in the ‘‘astrophobic’’ models proposed in Ref. [28], which we analyze in the next sections.

4 ΔN_{eff} in Astrophobic 2HDMs

We now discuss explicit models that realize astrophobic axions, i.e., axions with suppressed nucleon and electron couplings. In the previous section we have shown that a significant contribution to ΔN_{eff} can arise from sizable LFV axion couplings that are not in conflict with astrophysical and rare-decay constraints. Interestingly, astrophobic axions obtained in DFSZ-like models with two Higgs doublets necessarily imply PQ charges that are flavor non-universal [28]. In the following we discuss the structure of these models and calculate the resulting axion contribution to ΔN_{eff} .

There are four different models with two Higgs doublets (2HDM) that feature potentially nucleophobic QCD axions [28, 31]. The definition and the details of these scenarios, dubbed Q1-Q4, are given in Appendix D and summarized in Table D2. These models depend on the choice of a single vacuum angle $t_\beta \equiv \tan\beta$ (bounded by perturbativity), and the unitary rotations describing the transition between interaction and mass basis. They can be conveniently parametrized introducing

$$\xi_{ij}^{fP} \equiv (V_{fP})_{3i}^* (V_{fP})_{3j}, \quad (4.1)$$

with $f = u, d, e$, $P = L, R$, which depend on the unitary rotations $(V_{fP})_{ij}$ that diagonalize quark and charged lepton mass matrices. These parameters satisfy

$$0 \leq \xi_{ii}^{fP} \leq 1, \quad \sum_i \xi_{ii}^{fP} = 1, \quad |\xi_{ij}^{fP}| = \sqrt{\xi_{ii}^{fP} \xi_{jj}^{fP}}, \quad (4.2)$$

so that there are only two independent parameters in each fermion sector fP (ignoring complex phases). This also implies that there is no flavor violation if $\xi_{ii}^{fP} = 1$ for some $i = 1, 2, 3$.

Model	E_Q/N	C_c	C_s	C_t	C_b
Q1	14/3	2/3	-2/3	2/3	-2/3
Q2	8/3	2/3	1/3	-1/3	-2/3
Q3	8/3	-1/3	-2/3	2/3	1/3
Q4	2/3	-1/3	1/3	-1/3	1/3
Q5 (3HDM)	2	0	0	0	0

Table 1. Quark sectors in astrophobic 2HDM and 3HDM axion models after imposing conditions for nucleophobia, $C_u = 2/3$ and $C_d = 1/3$. For Q2 and Q3 additional choices has been made for quark flavor rotations, as explained in the text. Q5 can be realized only in 3HDMs.

Model	E_L/N	C_μ	C_τ	$C_{\tau e}$
E1	-2	-2/3	-1/3	2/3
E2	0	1/3	-1/3	2/3

Table 2. Lepton sectors in astrophobic 2HDM axion models after imposing conditions for nucleophobia, $C_u = 2/3$ and $C_d = 1/3$, electrophobia $C_e = 0$ and requiring $C_{\mu e} = 0$ in order to avoid stringent constraints from $\mu \rightarrow ea$ decays.

After imposing the condition for nucleophobia, $C_u = 2/3$ and $C_d = 1/3$, the resulting predictions for the remaining axion-quark couplings differ between the scenarios and we show representative models in Tables 1 that have been selected as follows. While for models Q1 and Q4 nucleophobia fixes all couplings, there is still some freedom in models Q2 and Q3, corresponding to the choice of quark flavor rotations. To avoid stringent bounds from flavor-violating meson decays, we only consider the case that flavor-violation in the quark sector is absent⁵, which leaves four models in each class (Q2 or Q3), only differing in predictions for 2nd and 3rd generation quark couplings. As these choices do not have much impact on our analysis, we simply choose two representative models for each class that we denote as Q2 and Q3 in Table 1 (this choice corresponds to $\xi_{33}^{uL} = \xi_{33}^{dL} = 1$ for model Q2, and $\xi_{22}^{uR} = \xi_{22}^{dR} = 1$ for model Q3).

In order to satisfy the astrophysical bounds on the axion-electron coupling for $f_a \lesssim 10^8$ GeV as needed for sizable ΔN_{eff} , the axion must also be electrophobic to good approximation. As discussed in Appendix D, within 2HDM there are essentially two potentially electrophobic scenarios⁶, dubbed E1 and E2, which are summarized in Table D4. Electrophobia ($C_e = 0$) is achieved through a tuning of flavor rotations, $\xi_{11}^{eL} \approx c_\beta^2 (s_\beta^2)$ for E1 (E2), and since nucleophobia requires $c_\beta^2 = 2/3$, there is necessarily lepton-flavor violation since $\xi_{11}^{eL} \neq 0, \xi_{11}^{eL} \neq 1$. In order to avoid strong constraints from $\mu \rightarrow ea$ decays, flavor violation cannot be present in the $\mu - e$ sector, which implies $\xi_{22}^{eL} \approx 0$ and thus large flavor-violating coupling in the $\tau - e$ sector, $C_{\tau e} \approx 2/3$. All non-zero axion-lepton couplings of the models E1 and E2, after imposing $C_e = C_{\mu e} = 0$, are summarized in Table 2. While both models

⁵This is a conservative assumption as far as ΔN_{eff} is concerned, since the presence of flavor-violating couplings can only increase ΔN_{eff} .

⁶There are four different models, but they differ only pairwise by the chiral structure of LFV couplings, which is irrelevant for our analysis.

predict the same value of $C_{\tau e} = 2/3$ and $C_\tau = -1/3$, the axion-muon coupling C_μ can be either $-1/3$ or $2/3$ depending on the model.

An astrophobic model is then obtained by combining any model in Table 1 with any model in Table 2, so in total there are eight such models, which we denote as e.g. Q1E1 with obvious notation. In Tables 1 and 2 we also list the contributions from each sector to the electromagnetic anomaly coefficient for each model, denoted by E_Q/N and E_L/N . The total contribution to the electromagnetic anomaly coefficient is given by the sum $E/N = E_Q/N + E_L/N$, for example model Q1E1 predicts $E/N = 8/3$. Simultaneous suppression of nucleon and electron couplings in the eight astrophobic 2HDMs then essentially fixes the flavor-violating axion coupling $C_{\tau e} \approx 2/3$, which dominates the contribution to ΔN_{eff} in all these models. We show the resulting prediction for ΔN_{eff} as a function of f_a in Fig. 2, where we also display the separate contributions to ΔN_{eff} from flavor-violating τ -decays and flavor-diagonal τ - and μ -scattering. Note that these contributions differ only between the two possible choices for the lepton sector, E1 and E2, giving the total lepton contribution to ΔN_{eff} that is denoted by solid lines (“total E1/E2”). There is also a small contribution from kaon scattering, giving the total contribution to ΔN_{eff} denoted by dash-dotted lines. Also shown is the Belle-II limit on flavor-violating τe couplings, which requires $f_a \gtrsim 2 \times 10^6$ GeV.

Although constraints on axion couplings to nucleons and electrons are avoided in these astrophobic models by construction, they are also subject to constraints on axion couplings to muons (from SN1987A) and photons (from HB stars⁷), shown as vertical lines in Fig. 2. The SN1987A bound only depends on the chosen lepton scenario, and allows for f_a as low as about 8×10^6 GeV (4×10^6 GeV) in E1 (E2). The constraint from HB stars is more stringent, and is controlled by the photon coupling, which can take only four different values (among the eight models) determined by $E/N \in \{14/3, 8/3, 2/3, -4/3\}$. In Fig. 2 we show the resulting bound on f_a for these four representative scenarios as vertical dashed brown lines, which varies from about 10^7 GeV (e.g. Q1E1) to 6×10^7 GeV (Q4E1). These limits are even more constraining than future Belle II searches for $\tau \rightarrow ea$ that will probe up to $f_a \sim 8 \times 10^6$ GeV. This implies that current constraints on f_a allow for ΔN_{eff} as large as 0.20 (0.22) for E2 (E1) models with $E/N = 8/3$, only considering leptonic production. However, for $f_a = \mathcal{O}(10^7)$ GeV contributions to ΔN_{eff} from axion-kaon scattering cannot be neglected, which arise from non-zero axion couplings to strange quarks. The maximal contribution from such scatterings is obtained for $C_s = 2/3$, which increases the total prediction for ΔN_{eff} for E2 (E1) models with $E/N = 8/3$ up to about 0.23 (0.25). For $f_a \gtrsim 5 \times 10^7$ GeV all models give essentially the same prediction for ΔN_{eff} , because only τ -decays are relevant for such large f_a . CMB-S4 will probe the parameter space up to $f_a \simeq 10^8$ GeV, which translates to $m_a \simeq 0.06$ eV, where the axion can indeed be considered relativistic at recombination to good approximation.

It is interesting to compare these expectations with complementary probes by future helioscopes such as BabyIAXO and IAXO. In Fig. 3 we show these prospects in the usual $(m_a, g_{a\gamma\gamma})$ plane, for the relevant f_a -window between 10^7 GeV and 10^9 GeV. The four

⁷Note that the CAST bound [58] is significantly weakened below $f_a \sim 10^8$ GeV.

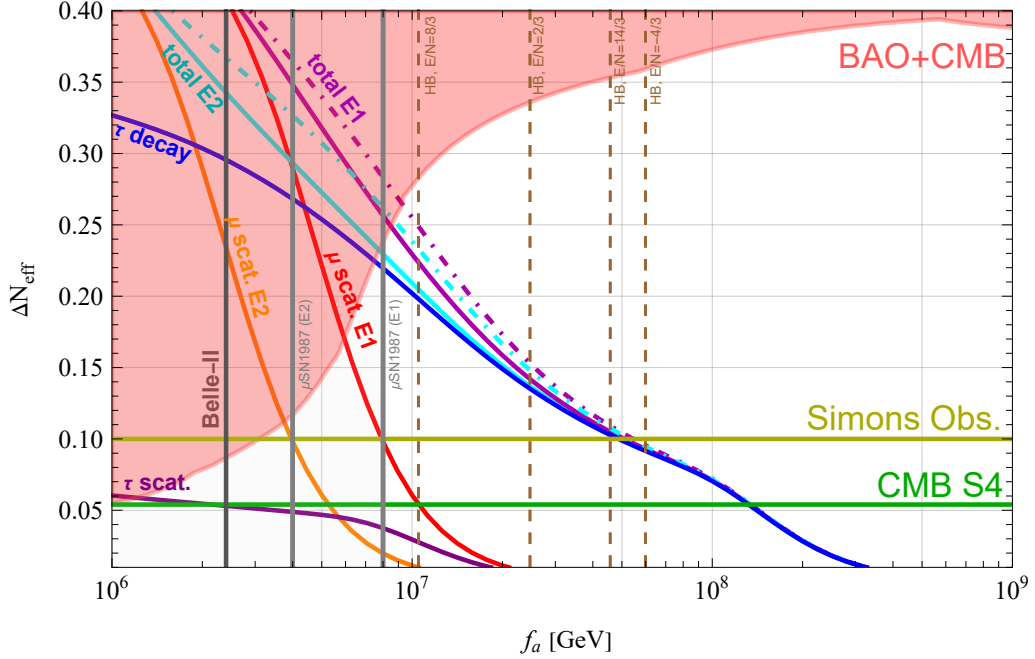


Figure 2. Additional effective number of neutrinos ΔN_{eff} as a function of f_a for astrophobic 2HDMs. Shown is total prediction for E1 (dark magenta) and E2 (light blue) models, without axion-kaon scatterings (solid lines) and with axion-kaon scatterings for $C_s = -2/3$ for $z = 0.49$ (dash-dotted lines). The difference in ΔN_{eff} between E1 and E2 models is entirely due to the different axion coupling to muons, which for E1 (E2) is $C_\mu = -2/3$ ($1/3$). Also shown are the predictions separately from $\tau \rightarrow e$ decays (blue), τ -scatterings (violet) and μ -scatterings, which differ between E1 (red) and E2 (orange). Vertical lines exclude the region to their left, and show constraints on the muon coupling from SN1987A [47] (grey), the Belle-II limit on $C_{\tau e}$ [54] (cyan) and the bound on C_γ from Horizontal Branch stars (HB) [49] (brown, dashed).

scenarios representing the predictions of astrophobic 2HDMs are denoted by black lines, and we show in brown the excluded region from HB star cooling constraints, the future projections for BabyIAXO (red) and IAXO (green) lines, and the contour lines for ΔN_{eff} in magenta (E1) and cyan (E2). BabyIAXO will constrain only models with $E/N = 14/3$ or $E/N = -4/3$, up to $f_a \simeq 10^8$ GeV, which roughly matches the reach expected from CMB-S4. IAXO instead will probe the same models down to $f_a \simeq 10^9$ GeV, way below the N_{eff} sensitivity. The other two scenarios with $E/N = 2/3$ and $E/N = 8/3$ have smaller photon couplings, and will be complementarily probed by IAXO and CMB-S4, reaching scales of $f_a \simeq 2 \times 10^8$ GeV and $f_a \simeq 8 \times 10^7$ GeV, respectively. Note, however, that for $m_a \gtrsim 0.2$ eV IAXO substantially loses its sensitivity to models with $E/N = 8/3$, and a small range of m_a up to about 0.5 eV will only be probed by future CMB surveys. Interestingly, also assuming that axions make up all dark matter in the Universe (which is possible even for $f_a \approx 10^7$ GeV in various cosmological scenarios with non-trivial evolution of the axion field [59–70]), the region inaccessible to IAXO will be covered by JWST [36] (see also Refs. [71–73]).

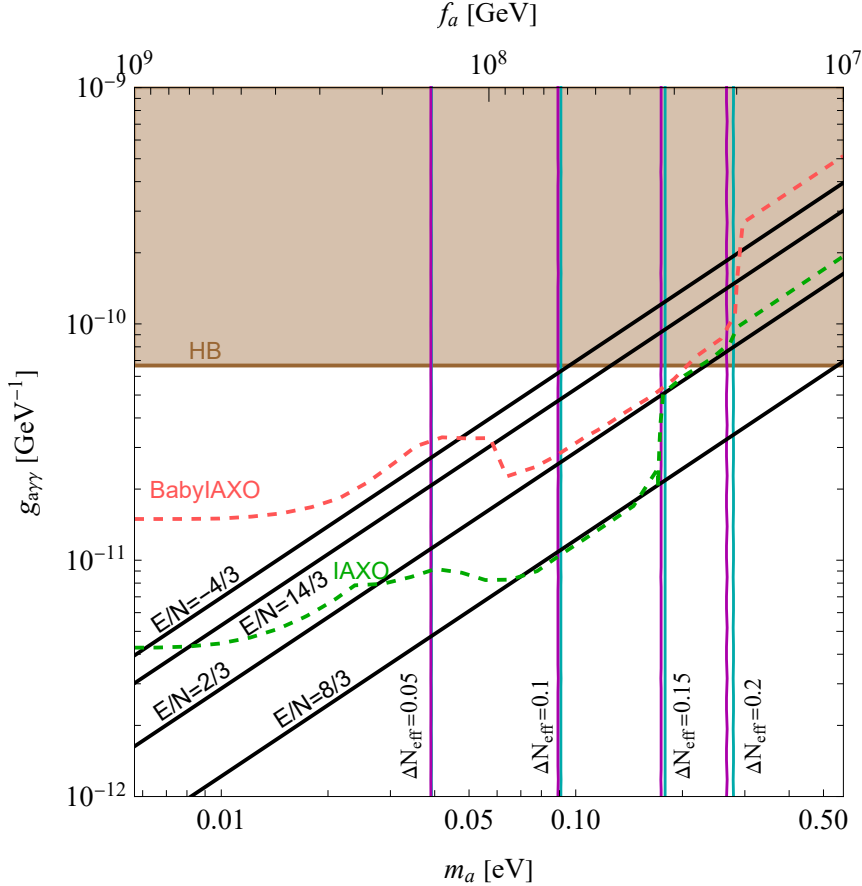


Figure 3. Predictions for the axion-photon coupling $g_{a\gamma\gamma}$ for the astrophobic models listed in Tables 1 and 2, characterised by the four indicated values of E/N . Magenta and cyan vertical lines indicate the total prediction for ΔN_{eff} (including axion-kaon scattering for $z = 0.49$) for E1 and E2 models, respectively. We denote in brown the region excluded by HB stars constraints, while the expected sensitivities of BabyIAXO and IAXO [35] will extend this region down to the contours plotted in dashed light red and green, respectively.

We close this section with a more detailed discussion of the various contributions to ΔN_{eff} in Fig. 2. Even though in 2HDM τ -decays dominate thermal axion production, the total ΔN_{eff} exceeds the value predicted when considering only such decays below $f_a = 3 \times 10^7$ GeV. Indeed there is a sub-leading contribution to axion production from μ -scatterings, which freeze-in axions after inverse τ -decays have frozen out. Axion production from τ -decays and μ -scatterings take place at different temperatures, affecting the abundance in a non-trivial way. In the left panel of Fig. 4 we show the leptonic rates in E1 models compared to the Hubble rate for a representative value of $f_a = 2 \times 10^7$ GeV. As anticipated, the τ -decay rate is large enough to keep axions in thermal equilibrium for $1 \lesssim x \lesssim 10$. The μ -scatterings instead are never effective enough to bring axions into thermal equilibrium, but still produce axions via freeze-in. On the right panel of Fig. 4 we show the evolution of the axion co-moving number density for the same benchmark value of $f_a = 2 \times 10^7$ GeV.

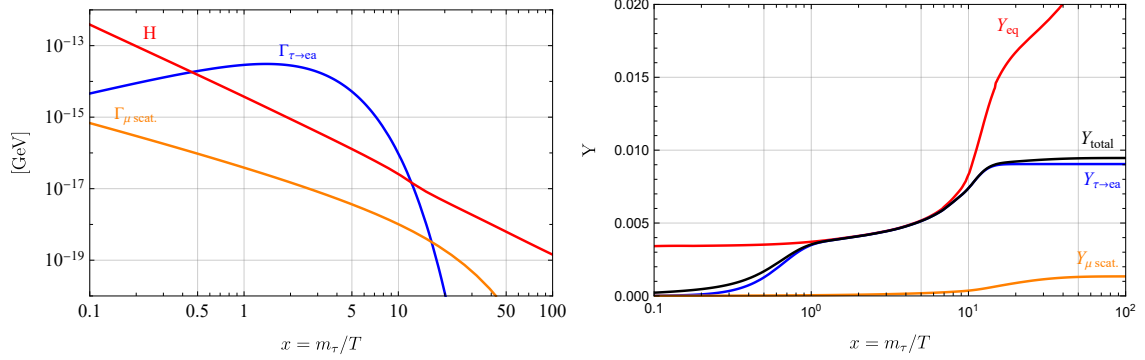


Figure 4. *Left panel:* Axion production rates from μ -scatterings (orange) and τ -decays (blue) as a function of $x = m_\tau/T$ compared to the Hubble rate (red) for E1 models ($C_\mu = -2/3$) at $f_a = 2 \times 10^7$ GeV. *Right panel:* Axion yield obtained by numerically solving the Boltzmann equation taking into account scattering and decays simultaneously (black) and separately (orange/green), compared to the equilibrium yield (red).

The rapid change in Y_{eq} is a result of the sudden changes in the number of relativistic degrees of freedom around the QCD phase transition at $x_{\text{QCDPT}} \approx 11$. As expected, the equilibrium yield is reached due to (inverse) τ -decays and ΔN_{eff} is determined by the freeze-out temperature $x \sim 15$. However, for $x > 15$ μ -scatterings become the main production channel, adding on top of the axion yield produced from τ -decays. Note however that the subsequent freeze-in is less effective than without τe -couplings, because the collision term is proportional to $Y_{\text{eq}} - Y$, and thus reduced as compared to the pure μ -scattering scenario due to the non-zero initial axion abundance. Hence, while axion freeze-in production solely from μ -scattering gives $\Delta Y \sim 1.5 \times 10^{-3}$, the same production subsequent to freeze-out production from τ -decays gives only $\Delta Y \sim 0.5 \times 10^{-3}$.

5 ΔN_{eff} in Astrophobic 3HDMs

In the previous section we have discussed non-universal DFSZ models with two Higgs doublets, which do not allow for suppressed axion couplings to muons or photons, in addition to nucleons and electrons. This is the reason why in those models f_a cannot be smaller than few times 10^7 GeV. As we will show now, this restriction can be avoided on the price of adding a third Higgs doublet, which admits $f_a \lesssim 10^7$ GeV without violating any astrophysical constraints. Most of these models can be probed by improved measurements of ΔN_{eff} , and require only a mild tuning to simultaneously suppress axion couplings to nucleons, electron and photons, in contrast to 2HDMs.

There are many 3HDMs giving astrophobic axions, and we refer for a detailed discussion to Appendix D. In this section we classify them according to the suppressed couplings relevant for avoiding astrophysical constraints: i) $|C_\mu| \ll 1$ ii) $|C_\gamma| \ll 1$, and iii) $|C_\mu|, |C_\gamma| \ll 1$ with LFV. The case of $|C_\mu|, |C_\gamma| \ll 1$ without LFV will be discussed in Sec. 6 in the context of the naturally astrophobic axion model. For each model we will

Model	E_L/N	C_μ	C_τ	$C_{\tau\mu}$
E1	-4/3	0	-2/3	0
E2	2/3	0	1/3	0
E3	0	0	0	0
E4	-8/3	-2/3	-2/3	0
E5	4/3	1/3	1/3	0
E6	-2/3	0	1/3	2/3

Table 3. Lepton sectors in astrophobic 3HDM axion models after imposing conditions for nucleophobia, $C_u = 2/3$ and $C_d = 1/3$ and electrophobia $C_e = 0$. In models E1 and E2, conditions for muonphobia $C_\mu = 0$ were additionally imposed. In models E1-E5, the conditions for nucleophobia, electrophobia and muonphobia (where possible) imply no LFV couplings. The E6 model is special as all three leptons carry different PQ charges.

compute the axion contribution to ΔN_{eff} as a function of f_a . All models are obtained by combining a quark sector model in Table D3 with a lepton sector model in Table D5, and require a single small PQ charge $X_0 \ll 1$ in order to be astrophobic. This can be achieved by choosing appropriate Higgs vacuum angles, $X_0 = (1 - 3c_1^2)c_2^2$ (cf. Eq. (D.35) and the discussion below), and the possible degree of suppression is only bounded by perturbativity of Yukawa couplings. Predictions for axion couplings in lepton sectors of astrophobic 3HDMs after imposing conditions for astrophobia are presented in Table 3. Note that E1 and E2 models in the context of 3HDMs give different predictions for axion couplings to leptons than E1 and E2 in the context of 2HDMs (cf. Table 2). The predictions for axion couplings to quarks are given in Table 1 and for Q1-Q4 are the same within 2HDMs and 3HDMs. There is a single new model in the context of 3HDMs, dubbed Q5.

5.1 Models with $|C_\mu| \ll 1$

We start with a discussion of models in which the axion coupling to muons is small, $|C_\mu| \ll 1$, but the axion-photon coupling is unsuppressed. In these models the PQ charges of leptons can have a $2 + 1$ flavor structure. There are 14 models of this type that are obtained by combining any of the 5 potentially nucleophobic models in the quark sector, summarized in Table D3, with either model E1, E2 or E3 in the charged lepton sector⁸, defined in Table D5, and taking $X_0 \ll 1$ and $\xi_{33}^{eL} = 1$, so that there is no LFV. Models involving E3 are special because all axion-lepton couplings vanish. The model Q5E3, in which also the axion-photon coupling is suppressed, will be discussed separately in Section 6. Nucleophobia and electrophobia can thus be obtained without flavor-violation, upon making appropriate choices for quark flavor rotations. Therefore the only leptonic contribution to ΔN_{eff} comes from the axion-tau coupling, which is fixed to be $C_\tau = -2/3$ in E1 and $C_\tau = 1/3$ in E2 models, respectively, and for E3 model even this contribution is absent.

The main difference between the five possible choices of quark sector models is the value of the axion-photon coupling. Taking into account all possible combinations with

⁸Model E6 instead has a 1+1+1 flavor structure and will be discussed below.

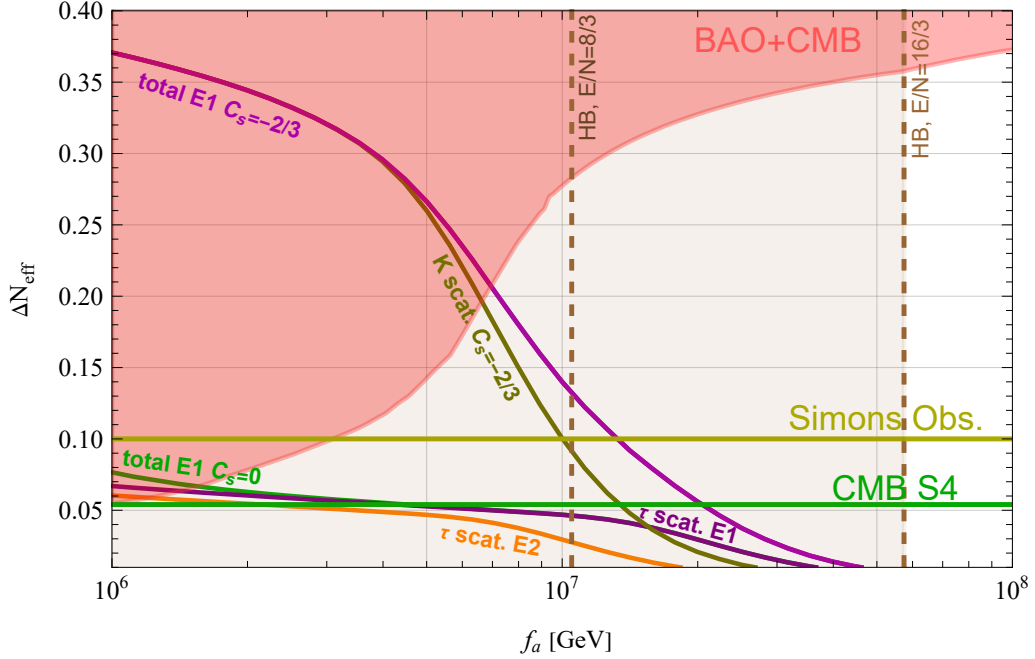


Figure 5. Additional effective number of neutrinos ΔN_{eff} as a function of f_a for astrophobic 3HDMs with $|C_\mu| \ll 1$. These models are obtained by combining E1, E2 and E3 with any model of the quark sector (Q1-Q5), and differ in their contributions to ΔN_{eff} only through the different values of C_τ and C_s . We only show the largest possible contribution represented by model Q3E1. The most important lower bound on f_a comes from HB star cooling bounds on the axion-photon coupling [49], which is strongest (weakest) for $E/N = 16/3(8/3)$.

the three lepton sector models, this coupling is determined by seven representative values, $E/N \in \{16/3, 14/3, 10/3, 8/3, 4/3, 2/3, -2/3\}$. These translate into a lower bound on f_a from HB constraints, which varies from about 10^7 GeV for the least constrained models with $E/N = 8/3$ (Q2E3, Q3E3, Q5E2) and $E/N = 4/3$ (Q2E1, Q3E1, Q4E2) to about 6×10^7 GeV for the most constrained model (Q1E2) with $E/N = 16/3$.

Since electron, muon, and LFV couplings are suppressed, the only leptonic contribution to ΔN_{eff} arises from scattering processes of τ -leptons, differing only between models E1 ($C_\tau = -2/3$), E2 ($C_\tau = 1/3$) and E3 ($C_\tau = 0$), and the resulting predictions are shown in Fig. 5. Taking into account the lower bounds on f_a from HB constraints as discussed above, this contribution is always below the sensitivity of CMB-S4. However, because there are no LFV couplings, the largest contribution to ΔN_{eff} in these models are actually due to kaon scattering, which is controlled by the value of the axion couplings to s -quarks. The value of this coupling can take just three different values, $C_s = 1/3$ or $C_s = -2/3$ in models Q1-Q4, while it vanishes in Q5. In Fig. 5 we show separately the predictions for ΔN_{eff} from tau and kaon scattering for two selected models in order to avoid clutter, which correspond to the smallest ($C_s = 0$ in Q5E1) and largest contributions from kaon scattering ($C_s = -2/3$ in e.g. Q3E1). The maximal contribution to ΔN_{eff} in these models, after taking into account the constraints on the axion-photon coupling, is 0.13 and within

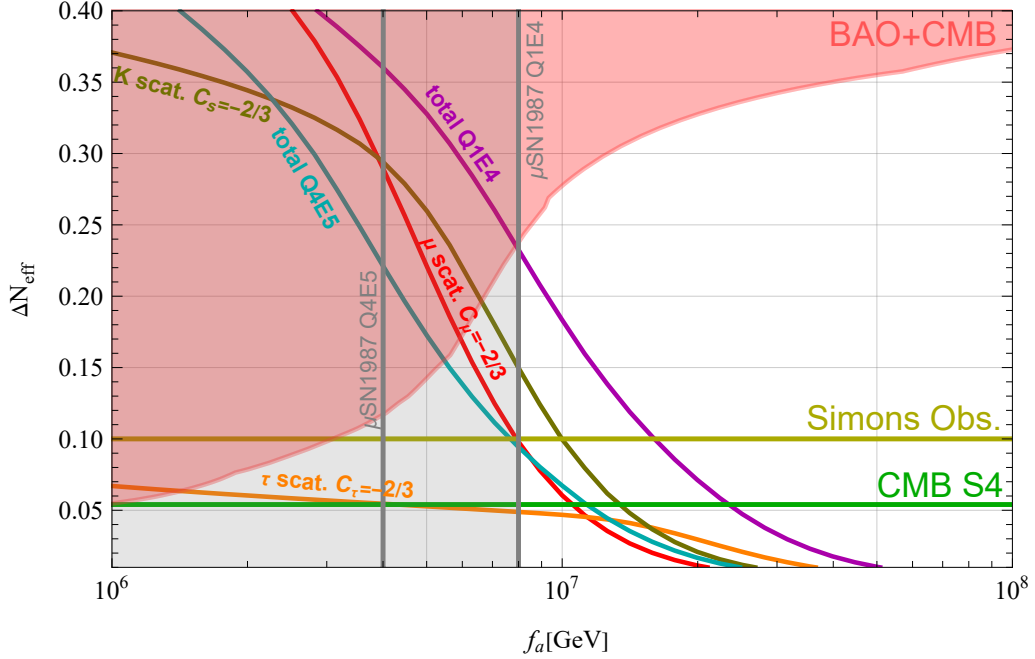


Figure 6. Additional effective number of neutrinos ΔN_{eff} as a function of f_a for astrophobic 3HDMs with $|C_\gamma| \ll 1$, which is realized in Q1E4 and Q4E5 models. The vertical grey line denotes the limit on the muon coupling from SN1987A [47], while red, brown and orange lines denote the contributions from scattering off muons, kaons and taus, respectively.

the reach of the Simons Observatory. However, the potential for improvement of the lower bound on f_a by future CMB experiments is quite limited and CMB-S4 will improve it up to 2×10^7 GeV (for models with maximal ΔN_{eff}), which is better than the astrophysical bound only for models with $E/N = 8/3$ or $4/3$. The other models will be probed more efficiently by IAXO or JWST than by CMB observations.

5.2 Models with $|C_\gamma| \ll 1$

Assuming a $2 + 1$ flavor structure of the (non-universal) PQ lepton charges, it is also possible to suppress the axion-photon coupling in 3HDMs. Indeed there are two models with $E/N = 2$ (Q1E4 and Q4E5), which allow for $f_a \sim \mathcal{O}(10^6)$ GeV without being in conflict with HB star cooling constraints. However, in these models axion-electron and axion-muon couplings cannot be suppressed simultaneously, as electrophobia implies $C_\mu = C_\tau = -2/3$ ($1/3$) in Q1E4 (Q4E5) model, which in turn requires $f_a \gtrsim 8(4) \times 10^6$ GeV from the SN1987A constraint on the axion-muon coupling. There is no LFV in these models, so that the only sizable contribution to ΔN_{eff} comes from axion-kaon, axion-muon, and axion-tau scatterings, and we show these contributions and the total prediction for ΔN_{eff} in Fig. 6. The predicted value of ΔN_{eff} in the Q1E4 model is larger than in the Q4E5 model, since the absolute values of axion couplings to muon, tau, and strange are twice as large in Q1E4 as compared to Q4E5. We see that the combined effect of these three

channels leads to ΔN_{eff} as large as 0.23 without violating the SN1987A constraint, which exceeds the maximal value that can be obtained in the models with $|C_\mu| \ll 1$ as discussed above, cf. Fig. 5. Interestingly, the current cosmological data set lower bounds on f_a in these models that are comparable to those from astrophysics. In Q4E5 the lower bound on f_a from thermal axion production is about 5×10^6 GeV so even slightly stronger than the SN1987A constraint. This is because for such small f_a the axion mass is around 1 eV, so the axion is not relativistic around recombination, which strengthens the upper bound on ΔN_{eff} . Due to relatively weak astrophysical constraints there are good prospects for testing both models in future CMB surveys. Model Q1E4 can be within the reach of the Simons Observatory (CMB-S4) for values of f_a up to 10^7 (2×10^7) GeV, while the reach for f_a in Q4E5 is weaker by about a factor two. Both models cannot be probed by IAXO due to the suppressed axion-photon coupling.

On the other hand, these models may still be probed by JWST, which for $f_a < 10^7$ GeV will be sensitive to the axion-photon couplings $g_{a\gamma\gamma} \equiv \alpha(2\pi f_a)^{-1}C_\gamma$ as small as $\mathcal{O}(10^{-11})$ [36]. However, whether JWST can really observe such axions depends on the contribution to C_γ from axion-pion mixing, which has rather large uncertainties. For the central value of this contribution $g_{a\gamma\gamma} \approx 10^{-11}$ for $f_a = 8 \times 10^6$ GeV, which is on the verge of the JWST sensitivity, but $g_{a\gamma\gamma}$ could be a factor of two larger when taking into account theoretical errors. Still, for $E/N = 2$ theoretical uncertainties allow for vanishing $g_{a\gamma\gamma}$ so definite conclusions cannot be made until the theory prediction has improved.

5.3 Models with $|C_\mu| \ll 1$ and $|C_\gamma| \ll 1$ and LFV

We finally discuss *proper* astrophobic models, where on top of nucleophobia and electrophobia also axion couplings to muons and photons are suppressed, so that *all* stellar cooling constraints are weakened. In such models, the dominant lower bound on f_a originates from the usual SN1987A constraint on axion-nucleon couplings, which are induced by higher-order corrections. Taking into account these corrections, the resulting lower bound on f_a can be as weak as 10^6 GeV, although the exact numerical value depends on the details of the axion model and is also sensitive to the uncertainties in the lattice determination of the ratio m_u/m_d [33].

As discussed in Appendix D, astrophobic models with $|C_\mu| \ll 1$ and $|C_\gamma| \ll 1$ can be constructed within the framework of DFSZ-like models with 3 Higgs doublets. There are three such models, depending on the PQ charge structure of charged leptons. Either the charges are universal, so that there is no LFV, or they are different for each generation, i.e., have a 1+1+1 flavor structure, indicating possibly large LFV. Here we focus first on the two proper astrophobic axion models with LFV, which have the best prospects to be probed by CMB observations in the near future, since flavor-violating τ -decays give the dominant contribution to ΔN_{eff} , in the absence of the axion-pion coupling. We will discuss the model with universal lepton charges (Q5E3) in the next section.

The two models are obtained by combining E6 in Table D5 with models Q2 or Q3 in Table D3 (dubbed Q2E6 and Q3E6, respectively), giving $E/N = 2$ and thus a suppressed axion coupling to photons. Proper astrophobia is obtained for $X_0 \ll 1$, giving for both models $C_e = C_\mu = 0$, $C_\tau = 1/3$, and the LFV coupling $C_{\tau\mu} = 2/3$. The largest contribu-

tion to ΔN_{eff} is due to axion production from τ -decays, but a sub-leading contribution is due to kaon scattering, which depends on the value of C_s that is controlled by quark flavor rotations, and can vary between $-2/3$ and $1/3$. In Fig. 7 we show the minimal total prediction for $C_s = 1/3$, as well as the contributions from kaon scattering and τ -decays alone. In contrast to the models discussed above, the constraint on f_a provided by cosmology, i.e., CMB and BAO data, is much stronger than limits from astrophysics or direct searches for LFV decays. Interestingly, despite the suppression of the axion-muon and axion-photon couplings, this only excludes values $f_a \lesssim 8 \times 10^6$ GeV. This is mainly due to the rather large production rate of thermal axions from $\tau \rightarrow \mu a$ decays, as well as the fact that for $f_a \lesssim 10^7$ GeV axions act as a warm dark matter and the upper bound on ΔN_{eff} rapidly tightens when decreasing f_a .

These models can be complementary probed by searches for $\tau \rightarrow \mu a$ at Belle-II [54]. While current bounds are not competitive with the constraints from cosmology, future runs of Belle-II are expected to probe f_a up to the level of 10^7 GeV, which corresponds to $\Delta N_{\text{eff}} \simeq 0.2$ for the models under consideration, and thus allow for complementarity to future CMB searches. Similarly to the models Q1E4 and Q4E5 with $|C_\gamma| \ll 1$ and unsuppressed axion-muon couplings discussed above (cf. Fig. 6), the JWST sensitivity strongly depends on the uncertainty of the theoretical prediction for the axion-photon coupling.

6 ΔN_{eff} from the Naturally Astrophobic QCD Axion

In this section, we discuss the naturally astrophobic axion model [33]. In this model, the SM Higgs is a nearly PQ charge eigenstate with a vanishing PQ charge, and the axion coupling to SM fermions is entirely controlled by their PQ charge assignments, so that no tuning of the parameters of the theory is required to achieve astrophobia.

In particular, a proper astrophobic model without LFV can be achieved by assigning the PQ charges of 2, 1, 0, and 0 to u , d , e , and μ , respectively, and assuming that the QCD and electromagnetic anomaly comes only from u and d . In the minimal scenario, the PQ charges of other SM fermions are zero. In the UV completion by 3HDM, this can be obtained by combining the flavor-universal model E3 in the charged lepton sector (see Table D5) with model Q5 in the quark sector, (see Table D3), upon taking $X_0 \ll 1$ and $\xi_{11}^{uR} = \xi_{11}^{dR} = 1$. This model, dubbed Q5E3, has a very interesting feature that the axion couples exclusively to u - and d -quarks, so that $X_0 \ll 1$ can be realized by strongly suppressing the vevs of the two non-SM Higgs fields consistent with perturbative unitarity, as these only give rise to up- and down-quark masses. This is in contrast to all other 3HDM models, where perturbativity of Yukawa couplings prevents this possibility, and instead require some (mild) tuning, see e.g. Ref. [30]. This model was proposed in Ref. [33], and it was shown that it can be UV-completed not only within the 3HDM scenarios but also by adding new vector-like quarks.

Both astrophysical constraints on f_a and the predictions for ΔN_{eff} somewhat depend on the particular UV completion. We show the prediction of ΔN_{eff} for the naturally astrophobic axion in various scenarios in Fig. 8. In the minimal model only up- and down-quarks

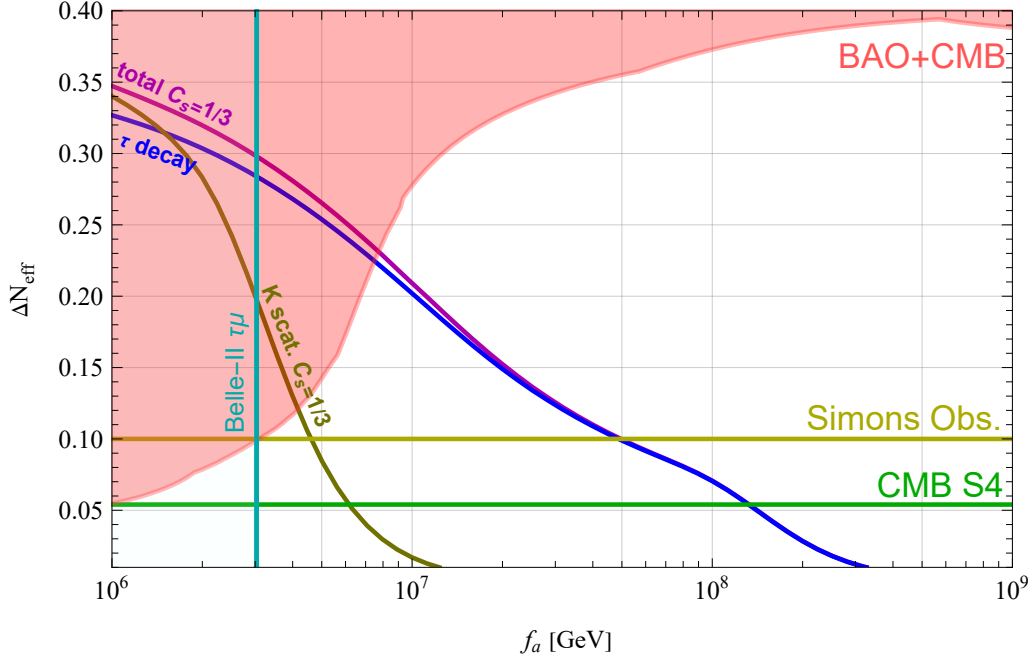


Figure 7. Additional effective number of neutrinos ΔN_{eff} as a function of f_a for proper astrophobic 3HDM with LFV, realized by the Q2E6 and Q3E6 models. The plot shows the prediction in the model with the smallest kaon contribution ($C_s = 1/3$) and $z = 0.49$. The maximal contribution for $C_s = -2/3$ to ΔN_{eff} is slightly larger, but the resulting current bound on f_a from cosmology is very similar. The vertical cyan line marks the lower bound on f_a from searches for flavor-violating $\tau \rightarrow \mu a$ decays at Belle-II [54].

couple to the axion and the corresponding couplings are $C_u = 2/3$ and $C_d = 1/3$. In the minimal model the astrophysical constraints on the axion-nucleon couplings allow for f_a as small as 10^6 GeV if $z \approx 0.49$ [33]. In this scenario axion couplings to pions, leptons and kaons are strongly suppressed, so the axion cannot be in thermal equilibrium below the QCD phase transition. Therefore, non-negligible contribution to ΔN_{eff} may only arise in the deconfined phase when the axion may be kept in thermal equilibrium by scattering with up- and down-quarks. The production rates of axions in these scattering processes with quarks are proportional to temperature, so the dominant production of axions occurs at low temperatures (since the Hubble scale scales as T^2). Hence, we expect that axions will be mostly produced for temperatures not far above the QCD phase transition. Unfortunately, the scattering rates for these processes cannot be reliably computed for such temperatures using perturbative methods [16] (see also Refs. [74, 75]). On the other hand, we know that astrophobic axions are not thermally produced in the regime when chiral perturbation theory correctly describes axion interactions. Thus, it is possible to estimate the maximal contribution to ΔN_{eff} that occurs if the axion decouples from SM plasma for temperatures around 150 MeV. However, if the production rate of axions is smooth it may well be that axions decouple at some higher temperature. For this reason in Fig. 8 we also show the relation between ΔN_{eff} and axion decoupling temperature using an instantaneous

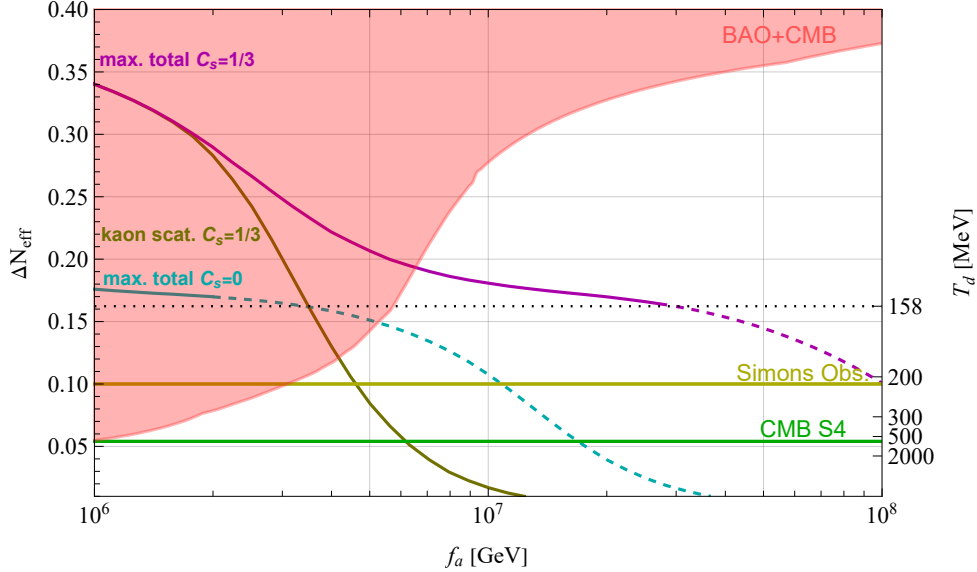


Figure 8. Additional effective number of neutrinos ΔN_{eff} as a function of f_a for the naturally astrophobic axion, realized e.g. by the E3Q5 model. Dotted lines indicate uncertainties due to the non-perturbative freeze-in. The axion-kaon scattering has been computed for $z = 0.49$ for which f_a down to few $\times 10^6$ GeV is consistent with astrophysical constraints. Axion decoupling temperatures T_d assuming prior equilibrium above the QCDPT are shown on right vertical axis.

decoupling approximation. We see that if the strong interactions keep the axion in thermal equilibrium for temperatures down to the QCD phase transition, ΔN_{eff} can be as large as about 0.15, while if it decouples around 1 GeV, ΔN_{eff} is around 0.05.

In Fig. 8 we also show the maximal value of ΔN_{eff} obtained by estimating the non-perturbative effects on axion production using the leading order up- and down-quark scattering rates above the QCD phase transition [17], setting the strong coupling g_s to 4π . We see that in the minimal scenario (corresponding to $C_s = 0$ in the plot), such scatterings are not able to thermalize axion unless f_a is below few $\times 10^6$ GeV. Nevertheless, freeze-in axion production via such scatterings may give non-negligible contribution to ΔN_{eff} resulting in the current lower bound from Planck around 5×10^6 GeV, which should be considered as an aggressive limit for the minimal model.

Given the uncertainty in the prediction of ΔN_{eff} one cannot use future CMB data to set robust bounds on the naturally astrophobic axion scenario. On the other hand, in case some deviation from ΛCDM model is found it may still be explained by the minimal model with $f_a = \mathcal{O}(10^7)$ GeV, but to reliably extract information about the axion from such data one would require a lattice determination of the axion temperature evolution.

The minimal model, where $C_d = 1/3$ and $C_s = 0$, requires additional model building (see Ref. [33]) to naturally suppress rare kaon decays induced by flavor-violating axion couplings in the s - d sector. Instead such decays are naturally suppressed without model building if $C_s = C_d$. For $C_s = 1/3$, the axion contribution to ΔN_{eff} is larger than in the minimal model for two reasons. First, the axion-kaon scattering is no longer suppressed

and results in a lower bound on f_a from Planck around 4×10^6 GeV, as seen from Fig. 8. Second, axion production from strange-quark scattering is expected to be bigger than that from up- and down-quark scattering due to much larger strange-quark mass. Using the same estimate for the non-perturbative contribution as above, we found that strange-quark scattering can keep the axion in thermal equilibrium for temperatures down to the QCD phase transition for f_a exceeding even 10^7 GeV. This results in a lower bound on f_a from Planck about 7×10^6 GeV, as seen in Fig. 8.

We have also checked that the lower bound of $f_a \gtrsim 7 \times 10^6$ GeV from Planck is independent of the choice for estimating the non-perturbative axion production. For example, the bound stays the same if one takes $g_s = \sqrt{4\pi}$ instead of 4π . Also the estimate proposed in Ref. [16] with the thermally averaged rate parameterized as $\bar{\Gamma} = \kappa T^3/f^2$ for temperatures between 2 GeV and the QCD phase transition with $\kappa = 0.1$ or 0.01 gives the same lower bound on f_a . In all these estimates the axion is thermalized down to the QCD phase transition for $f_a = \mathcal{O}(10^7)$ GeV, which is the reason why the exact value of the rate has no impact on the predicted value of ΔN_{eff} . On the other hand, the estimates for the sensitivity of future experiments are much less robust. For example, the reach of the Simons Observatory for f_a varies between 10^7 and 10^8 GeV if one changes g_s from $\sqrt{4\pi}$ to 4π in our estimate for strange-quark scattering.

Let us also comment on the fact that for $C_s = 1/3$ the astrophysical bounds on the axion-nucleon couplings can allow for f_a much below 10^7 GeV only if axion couplings to charm and/or bottom are also $\mathcal{O}(1)$ [33]. We have checked that turning on these couplings does not affect the current lower bound on f_a . This is because axion production from charm- and bottom-quark scattering is Boltzmann suppressed around the QCD phase transition, and also because strange-quark scattering alone is sufficient to thermalize axions down to the QCD phase transition.

We emphasize that the naturally astrophobic axion is the model that is least constrained by the CMB, and f_a much below 10^7 GeV may be consistent with all available data. Such values of f_a imply an axion mass $\mathcal{O}(1)$ eV, so it is non-relativistic at recombination. Thus, in this scenario ΔN_{eff} is just a useful parametrization of the energy density of thermal axions and axions act like warm dark matter rather than constituting extra relativistic degree of freedom, which is yet another feature that could help to distinguish the naturally astrophobic axion from other axion models using future CMB data.

Our results also have implications to minimal axiogenesis [76]. In the minimal axiogenesis scenario, the PQ symmetry-breaking field rotates in field space in the early universe, which corresponds to a non-zero PQ charge. The PQ charge is transferred to baryon asymmetry via axion-SM couplings and electroweak sphaleron processes. For $f_a \gg 10^7$ GeV, however, the produced baryon asymmetry is smaller than the observed one after imposing the constraint from overproduction of axion dark matter by the kinetic misalignment mechanism [67], unless some of the axion-SM couplings are much larger than the $1/f_a$ -suppressed one. For $f_a \lesssim 10^7$ GeV, on the other hand, the observed baryon asymmetry can be explained without introducing large couplings. Even with the maximal possible scattering rate of the axion with u - and d -quarks or $C_s = 1/3$, the current constraints from the CMB and BAO can be satisfied. If the scattering rates with quarks become as large

as those with $g_s \sim 4\pi$ before the QCD phase transition, CMB-S4 can probe the parameter space of the successful minimal axiogenesis without large couplings.

Even though axion-photon coupling in this scenario is smaller by at least one order of magnitude than in models with $E/N \neq 2$, it may be still possible for JWST to discover a DM axion with mass of $\mathcal{O}(1)$ eV. Thus, using complementarity of future CMB and JWST observations, it will be viable to pin down axions that are responsible both for DM and baryogenesis.

7 Conclusions

We have investigated thermal production of QCD axions in so-called astrophobic models in which astrophysical constraints on the axion decay constant are relaxed. A model-independent feature of such models is that the axion-pion coupling is so small that the impact of axion-pion scattering on the production of thermal axions is negligible. However, we found that a large abundance of hot axions, parameterised by the extra effective number of neutrinos ΔN_{eff} , can be sizable in the presence of other axion couplings, such as couplings to muons, strange-quarks or LFV couplings leading to axion production from $\tau \rightarrow \ell a$ decays, see Fig. 1.

The simplest astrophobic axion models are generalized DFSZ models with two Higgs doublets with flavor non-universal PQ charges [28]. In this class of models, suppression of axion couplings to nucleons and electrons fixes the size of LFV couplings, which directly control $\tau \rightarrow e a$ decays and give a sharp prediction for ΔN_{eff} as a function of f_a . However, axion-photon couplings are unsuppressed and a lower bound on f_a arises from HB star cooling constraints, which varies between $(1 \div 6) \times 10^7$ GeV, depending on the model. This in turn limits the predicted ΔN_{eff} to be below about $(0.1 \div 0.25)$ (see Fig. 2), which are within the reach of the Simons Observatory. This is in sharp contrast to the predictions of the minimal DFSZ and KSVZ axion models, where ΔN_{eff} is at most 0.03 in the region of f_a consistent with astrophysical constraints, and it is difficult to observe such small ΔN_{eff} in the foreseeable future. The range of f_a leading to large ΔN_{eff} in astrophobic 2HDM will be also probed by axion helioscopes. Two of the models are within the reach of BabyIAXO, while the remaining ones can only be probed by IAXO. A small range of $f_a \lesssim 3 \times 10^7$ GeV will not be covered by IAXO, but it is within reach of JWST, if one assumes that axions make up all dark matter in the Universe.

We have also constructed generalized DFSZ models with three Higgs doublets. In such models there is more flexibility in the structure of axion couplings as compared to 2HDMs. In particular, it is possible to suppress nucleon and electron couplings without additional tuning. In such models ΔN_{eff} is typically much smaller than in 2HDMs, because flavor-conserving axion-lepton scatterings are not as efficient in producing thermal axions. However, we found that in such models axion-kaon scatterings may still lead to large ΔN_{eff} . This effect is particularly important in models with axion-photon couplings small enough to allow for f_a down to 10^7 GeV, and the resulting ΔN_{eff} can even be above 0.1, within the reach of the Simons Observatory (see Fig. 5).

In order to allow for f_a below 10^7 GeV consistent with astrophysical constraints, it is necessary to not only arrange for $E/N = 2$, which accidentally relaxes the lower bound on f_a from HB stars to about 10^6 GeV, but also to suppress the axion-muon coupling in order to avoid constraints from SN1987A. In such models, ΔN_{eff} sets a lower bound on f_a much stronger than the astrophysical constraints, if efficient axion production from flavor-violating τ -decays or axion-kaon scattering is possible. We constructed such models and found a lower bound on f_a given by 8×10^6 GeV (see Fig. 7).

We also have investigated the recently proposed naturally astrophobic QCD axion model. We found that in the minimal model where the axion couples to the SM only via the up and down quarks, the axion cannot be kept in thermal equilibrium with the SM plasma for temperatures below the QCD phase transition, due to strongly suppressed axion couplings to pions, kaons, and leptons. However, axions may still be produced thermally before the QCD phase transition in scatterings with free quarks. The production rates for such processes cannot be reliably computed using perturbative techniques, and the maximal value of ΔN_{eff} can only be estimated. If the axion decouples exactly at the QCD phase transition, current cosmological constraints lead to a lower bound $f_a \gtrsim 6 \times 10^6$ GeV, which can be even further weakened using more conservative assumptions about the axion decoupling temperature. Thus, in the naturally astrophobic axion model both astrophysical and cosmological constraints allow minimal axiogenesis to explain both the observed DM and the baryon abundance. Future CMB surveys may probe the parameter space relevant for this scenario, where the axion mass can be as large as 1 eV. The axion-photon coupling may be large enough to lead to a discovery of axion DM by JWST, and future CMB data could be used to cross-check such an interpretation.

Acknowledgments

We would like to thank Luca di Luzio, Ricardo Ferreira, Maxim Laletin, Fabrizio Rompineve and Giovanni Villadoro for useful discussions and correspondence. M.B. and R.Z. thank the Galileo Galilei Institute for Theoretical Physics and INFN for hospitality and partial support during the completion of this work. This work was partially supported by the National Science Centre, Poland, under research grant no. 2020/38/E/ST2/00243 (M.B. and M.L.), has received support from the European Union’s Horizon 2020 research and innovation programme under the Marie Skłodowska-Curie grant agreement No 860881-HIDDeN, is partially supported by project C3b of the DFG-funded Collaborative Research Center TRR257 “Particle Physics Phenomenology after the Higgs Discovery” (R.Z.), and is partially supported by Grant-in-Aid for Scientific Research from the Ministry of Education, Culture, Sports, Science, and Technology (MEXT), Japan (20H01895) and by World Premier International Research Center Initiative (WPI), MEXT, Japan (Kavli IPMU) (K.H.). M.L. thanks the Karlsruhe Institute of Technology (KIT) for hospitality.

A Axion Couplings to Pions and Kaons

An anomalous axial rotation of light quarks $q = (u, d, s)^T$ parametrized by Q_a

$$q \rightarrow e^{i\gamma_5 \frac{a}{2f_a} Q_a} q, \quad (\text{A.1})$$

which for $\text{Tr}Q_a = 1$ cancels the $aG\tilde{G}$ term, induces an axion dependence in the quark masses

$$M_a = e^{ia(x)Q_a/2f_a} M_q e^{ia(x)Q_a/2f_a}, \quad (\text{A.2})$$

where $M_q = \text{diag}(m_u, m_d, m_s)$. The relevant Lagrangian involving axion and u, d, s quarks is given by

$$\mathcal{L} = \sum_{q=u,d,s} \frac{(C_q - Q_a^q)}{2f_a} (\partial_\mu a) \bar{q} \gamma^\mu \gamma_5 q - \sum_q \bar{q} M_a q, \quad (\text{A.3})$$

We can make the usual choice $Q_a = M_q^{-1}/\text{Tr}M_q^{-1}$, which avoids axion-pion mixing. Explicitly, this results in the following form of the matrix

$$Q_a = \begin{pmatrix} \frac{1}{1+z+w} & 0 & 0 \\ 0 & \frac{z}{1+z+w} & 0 \\ 0 & 0 & \frac{w}{1+z+w} \end{pmatrix}, \quad (\text{A.4})$$

with $z = m_u/m_d$ and $w = m_u/m_s$. On the other hand, the LO chiral lagrangian is given by [5, 77]

$$\mathcal{L} = \frac{f_\pi^2}{4} \left(\text{Tr}(D^\mu U^\dagger D_\mu U) + 2B \text{Tr}(UM_a^\dagger + M_a U^\dagger) \right) + \frac{\partial_\mu a}{2f_a} c_a \text{Tr} \left(\frac{if_\pi^2}{2} \lambda_a (U \partial^\mu U^\dagger - U^\dagger \partial^\mu U) \right), \quad (\text{A.5})$$

where

$$U = \exp \left(\frac{i}{f_\pi} \begin{pmatrix} \pi^0 + \eta/\sqrt{3} & \sqrt{2}\pi^+ & \sqrt{2}K^+ \\ \sqrt{2}\pi^- & -\pi^0 + \eta/\sqrt{3} & \sqrt{2}K^0 \\ \sqrt{2}K^- & \sqrt{2}\bar{K}^0 & -2\eta/\sqrt{3} \end{pmatrix} \right), \quad (\text{A.6})$$

and

$$c = \begin{pmatrix} C_u - Q_u^a & 0 & 0 \\ 0 & C_d - Q_d^a & 0 \\ 0 & 0 & C_s - Q_s^a \end{pmatrix} \quad (\text{A.7})$$

$$= \frac{1}{3} \text{Tr}(c) \mathbf{1} + \frac{1}{2} \text{Tr}(c\lambda_3) \lambda_3 + \frac{1}{2} \text{Tr}(c\lambda_8) \lambda_8 = c_a \lambda_a,$$

is the shifted axial coupling matrix, which can be decomposed as a linear combination of Gell-Mann matrices and the unit matrix. After choosing Q_a according to Eq. (A.4), the whole axion dependence is moved to the axial current and the mass terms. One can find the axion mass in 3-flavor ChPT in leading order in w as

$$m_a^2 = \frac{f_\pi^2 m_\pi^2 (4z(1+z) + w(1-z)^2)}{4f_a^2 (1+z)^2 (1+z+w)}. \quad (\text{A.8})$$

A.1 Coupling to Pions

One can show that the trace argument of axial current for pions, keeping up to 3 fields, is given by

$$U\partial^\mu U^\dagger - U^\dagger\partial^\mu U = \frac{4i}{3f_\pi^3} \left(\partial_\mu \pi^b (\pi\pi) - \pi^b (\pi\partial_\mu \pi) \right) \lambda^b, \quad (\text{A.9})$$

where now the index b is restricted to $SU(3)$ generators contracted with pions, that is, $b = 1, 2, 3$. Using $\text{Tr}\lambda^a\lambda^b = 2\delta^{ab}$, axion-pion couplings are given by

$$\mathcal{L}_{\text{axial}} = -\frac{2}{3} \frac{\partial_\mu a}{f_a f_\pi} c_a \left(\partial_\mu \pi^b (\pi\pi) - \pi^b (\pi\partial_\mu \pi) \right) \delta^{ab}. \quad (\text{A.10})$$

Taking into account the Kronecker- δ with restricted index b and Eq. (A.7), we have $c_a \delta_{a3} = c_3$, which can be further evaluated to $\text{Tr}(c\lambda_3)/2 = (C_u - Q_u^a - C_d + Q_d^a)/2$. Note that these terms are independent of C_s . After further simplifications we end up with

$$\mathcal{L}_{\text{axial}} = -\frac{C_u - C_d - Q_u^a + Q_d^a}{3f_\pi f_a} (\partial_\mu a) \left(2\partial_\mu \pi_0 \pi_+ \pi_- - \pi_0 \partial_\mu \pi_+ \pi_- - \pi_0 \pi_+ \partial_\mu \pi_- \right). \quad (\text{A.11})$$

Identifying the prefactor rescaled by $f_\pi f_a$ as the axion-pion coupling and using the explicit form of Q_a from Eq. (A.4), we obtain the known result [37]

$$C_\pi = -\frac{1}{3} \left(C_u - C_d - \frac{1-z}{1+z+w} \right). \quad (\text{A.12})$$

In astrophobic axion models $C_u = 2/3$, $C_d = 1/3$ and for approximate values $z \approx 1/2$ and $w \approx 0$ the pion coupling vanishes. Since scatterings with pions are the leading contribution to the abundance of thermal axions in generic models, $z \neq 1/2$ and $w \neq 0$ may play a role in determination of ΔN_{eff} . However, as we have checked for the parameter space consistent with astrophysical constraints on the axion-nucleon, the production via scatterings with pions always contributes to ΔN_{eff} less than 0.01, far beyond the reach of future experiments.

A.2 Coupling to Kaons

In the physical basis, with the choice of Q_a given by Eq. (A.4), we move the axion interaction (up to order $1/f_a^2$ corrections) to the axial current. The only non-zero contribution to the axion kaon coupling comes from the axial current in Eq. (A.5) and for values $z = 1/2$, $w = 0$ has the form

$$\begin{aligned} \mathcal{L}_{aK} = & -\frac{\partial_\mu a}{36f_a f_\pi} \left(-3 \left(C_u - C_d - \frac{1}{3} \right) \left(3\sqrt{2}K^+ \pi^- \partial^\mu \bar{K}^0 - 3\sqrt{2}K^0 \pi^+ \partial^\mu K^- + \bar{K}^0 \pi^0 \partial^\mu K^0 \right. \right. \\ & - 3\sqrt{2}\bar{K}^0 \pi^- \partial^\mu K^+ - 2\bar{K}^0 K^0 \partial^\mu \pi^0 + 3\sqrt{2}K^- \pi^+ \partial^\mu K^0 + K^- \pi^0 \partial^\mu K^+ \\ & \left. \left. - 2K^- K^+ \partial^\mu \pi^0 + \pi^0 K^0 \partial^\mu \bar{K}^0 + \pi^0 K^+ \partial^\mu K^- \right) \right. \\ & + 3 \left(C_u + C_d - 1 - 2C_s \right) \left(K^0 \pi^0 \partial^\mu \bar{K}^0 - \sqrt{2}K^+ \pi^- \partial^\mu \bar{K}^0 - K^+ \pi^0 \partial^\mu K^- \right. \\ & + \sqrt{2}K^0 \pi^+ \partial^\mu K^- + \bar{K}^0 \pi^0 \partial^\mu K^0 - \sqrt{2}\bar{K}^0 \pi^- \partial^\mu K^+ - 2\bar{K}^0 K^0 \partial^\mu \pi^0 \\ & + 2\sqrt{2}\bar{K}^0 K^+ \partial^\mu \pi^- - \sqrt{2}K^- \pi^+ \partial^\mu K^0 + K^- \pi^0 \partial^\mu K^+ - 2K^- K^+ \partial^\mu \pi^0 \\ & \left. \left. - 2\sqrt{2}K^- K^0 \partial^\mu \pi^+ \right) \right). \end{aligned} \quad (\text{A.13})$$

For astrophobic axions with charges $C_u = 2/3$, $C_d = 1/3$, $C_s \neq 0$, for which the charge matrix Eq. (A.7) is $c = \text{diag}(0, 0, C_s)$, only the contribution from strange quark coupling remains

$$\begin{aligned} \mathcal{L}_{aK} = \frac{C_s}{6f_a f_\pi} \partial_\mu a \Big(& \bar{K}^0 (\pi^0 \partial^\mu K^0 - 2K^0 \partial^\mu \pi^0 - \sqrt{2}\pi^- \partial^\mu K^+ + 2\sqrt{2}K^+ \partial^\mu \pi^-) - \\ & - K^- (\sqrt{2}\pi^+ \partial^\mu K^0 - 2\sqrt{2}K^0 \partial^\mu \pi^+ + \pi^0 \partial^\mu K^+ - 2K^+ \partial^\mu \pi^0) + \\ & + K^0 \pi^0 \partial^\mu \bar{K}^0 - \sqrt{2}K^0 \pi^+ \partial^\mu K^- - \sqrt{2}K^+ \pi^- \partial^\mu \bar{K}^0 - K^+ \pi^0 \partial^\mu K^- \Big). \end{aligned} \quad (\text{A.14})$$

Note that those couplings are not suppressed in contrast to the axion-pion coupling. As a result, the suppression of the kaon scattering rate comes solely from the Boltzmann factors and is insufficient to completely remove the kaon contribution to axion thermalization. The axion also couples to one η and two kaons, but the scattering rate is further suppressed by Boltzmann factors.

B Axion Production Rates

In this appendix we collect useful expressions for calculating thermal axion production rates, mainly following Ref. [78].

B.1 Equilibrium Number Densities

The number density of particles in thermal equilibrium is given by

$$n_i^{\text{eq}} = g_i \int \frac{d^3k}{(2\pi^3)} f_i^{\text{eq}} \simeq \frac{g_i}{2\pi^2} m_i^2 T K_2\left(\frac{m_i}{T}\right), \quad (\text{B.1})$$

where g_i denotes the number of internal degrees of freedom and $f_i^{\text{eq}} = 1/(e^{-E_i/T} \pm 1)$ denotes the phase space distributions with $E_i = (\vec{k}^2 + m_i^2)^{1/2}$. One can approximate the equilibrium distributions for both bosons and fermions by a Maxwell-Boltzmann distribution, $f_i^{\text{eq}} \simeq \exp(-E_i/T)$. This allows to approximate the number densities by the last equality, where $K_2(m_i/T)$ denotes the modified Bessel function of second kind with asymptotic behaviour

$$K_2(x) = \begin{cases} 2/x^2 & x \ll 1 \\ e^{-x} \sqrt{\pi/2x} & x \gg 1 \end{cases}. \quad (\text{B.2})$$

The axion mass is negligible while being thermally produced. We use the exact Bose-Einstein distribution with equilibrium density

$$n_a^{\text{eq}} = \frac{\zeta(3)}{\pi^2} T^3. \quad (\text{B.3})$$

B.2 Collision Operators and Production Rates

Axion production rates are related to the collision operator in the Boltzmann equation by $\Gamma_i(T) = \mathcal{C}_i/n_a^{\text{eq}}$, where i collectively denotes scattering processes $p_1 p_2 \leftrightarrow p_3 a$ and decays $p_1 \leftrightarrow p_2 a$. For scatterings the collision operator given by (neglecting Pauli blocking)

$$\mathcal{C}_{p_1 p_2 \leftrightarrow p_3 a} = \int d\Pi_1 d\Pi_2 d\Pi_3 d\Pi_a f_1^{\text{eq}} f_2^{\text{eq}} (2\pi)^4 \delta^4(p_1 + p_2 - p_3 - p_a) |\mathcal{M}_{p_1 p_2 \rightarrow p_3 a}|^2, \quad (\text{B.4})$$

where p_i denotes to the momentum of the i th particle, $d\Pi_i = d^3p_i/2E_i(2\pi)^3$ is the Lorentz invariant phase space measure, and $|\mathcal{M}_{p_1p_2 \rightarrow p_3a}|^2$ denotes the squared matrix element of the scattering process including sums over initial and final polarizations (no averaging). The collision operator can be related to the cross section

$$\sigma_{p_1p_2 \rightarrow p_3a} = \frac{1}{g_1g_2} \frac{1}{4p_1 \cdot p_2 v_{12}} \int d\Pi_3 d\Pi_a (2\pi)^4 \delta^4(p_1 + p_2 - p_3 - p_a) |\mathcal{M}_{p_1p_2 \rightarrow p_3a}|^2, \quad (\text{B.5})$$

where g_1, g_2 are the internal degrees of freedom of the initial particles and v_{12} is their Lorentz invariant relative velocity, given by

$$v_{12} = \frac{\sqrt{(p_1 \cdot p_2)^2 - m_1^2 m_2^2}}{2p_1 \cdot p_2} = \frac{s}{2p_1 \cdot p_2} \lambda^{1/2} \left(\frac{m_1}{\sqrt{s}}, \frac{m_2}{\sqrt{s}} \right), \quad (\text{B.6})$$

with $\lambda(x, y) = [1 - (x + y)^2][1 - (x - y)^2]$. This gives

$$\mathcal{C}_{p_1p_2 \leftrightarrow p_3a} = 2g_1g_2 \int d\Pi_1 d\Pi_2 f_1^{\text{eq}} f_2^{\text{eq}} \lambda^{1/2}(x_1, x_2) s \sigma_{p_1p_2 \rightarrow p_3a}(s), \quad (\text{B.7})$$

where $x_i = m_i/\sqrt{s}$ and the dependence on initial state momenta is encoded in the center-of-mass energy s . Changing integration variables and performing one integration in the Boltzmannian limit $f_i^{\text{eq}} \simeq \exp(-E_i/T)$ leaves a single integral over the center-of-mass energy

$$\mathcal{C}_{p_1p_2 \leftrightarrow p_3a} = \frac{g_1g_2}{32\pi^4} T \int_{s_{\min}}^{\infty} \lambda(x_1, x_2) s^{3/2} \sigma_{p_1p_2 \rightarrow p_3a}(s) K_1 \left(\frac{\sqrt{s}}{T} \right) ds, \quad (\text{B.8})$$

where $s_{\min} = \max\{(m_1+m_2)^2, (m_3+m_a)^2\}$, and $K_1(x)$ denotes the modified Bessel function of second kind with asymptotic behaviour

$$K_1(x) = \begin{cases} 1/x & x \ll 1 \\ e^{-x} \sqrt{\pi/2x} & x \gg 1 \end{cases}. \quad (\text{B.9})$$

This collision term is conveniently rewritten in terms of the thermally averaged cross-section as

$$\mathcal{C}_{p_1p_2 \leftrightarrow p_3a} = n_1^{\text{eq}} n_2^{\text{eq}} \langle \sigma_{p_1p_2 \rightarrow p_3a} v \rangle, \quad (\text{B.10})$$

which defines the latter as (in the Boltzmannian limit)

$$\langle \sigma_{p_1p_2 \rightarrow p_3a} v \rangle = \frac{1}{8m_1^2 m_2^2 T K_2(m_1/T) K_2(m_2/T)} \int_{s_{\min}}^{\infty} \lambda(x_1, x_2) s^{3/2} \sigma_{p_1p_2 \rightarrow p_3a}(s) K_1 \left(\frac{\sqrt{s}}{T} \right) ds. \quad (\text{B.11})$$

If one of the initial particles (particle 2) can be considered massless to good approximation, $m_2 \rightarrow 0$, this simplifies to

$$\langle \sigma_{p_1p_2 \rightarrow p_3a} v \rangle|_{m_2=0} = \frac{1}{16m_1^2 T^3 K_2(m_1/T)} \int_{s_{\min}}^{\infty} \left(1 - \frac{m_1^2}{s} \right)^2 s^{3/2} \sigma_{p_1p_2 \rightarrow p_3a}(s) K_1 \left(\frac{\sqrt{s}}{T} \right) ds. \quad (\text{B.12})$$

If the initial particles have the same mass, one has

$$\langle \sigma_{p_1 p_2 \rightarrow p_3 a} v \rangle |_{m_2=m_1} = \frac{1}{8m_1^4 T K_2(m_1/T)^2} \int_{s_{\min}}^{\infty} \left(1 - \frac{4m_1^2}{s}\right) s^{3/2} \sigma_{p_1 p_2 \rightarrow p_3 a}(s) K_1\left(\frac{\sqrt{s}}{T}\right) ds. \quad (\text{B.13})$$

The axion production rate from scattering processes is finally given by

$$\Gamma_{p_1 p_2 \rightarrow p_3 a}(T) = \frac{n_1^{\text{eq}} n_2^{\text{eq}}}{n_a^{\text{eq}}} \langle \sigma_{p_1 p_2 \rightarrow p_3 a} v \rangle, \quad (\text{B.14})$$

and for the total production rate from scattering $\Gamma_S(T)$ all processes have to be summed

$$\Gamma_S(T) = \sum_{p_1, p_2} \Gamma_{p_1 p_2 \rightarrow p_3 a}(T). \quad (\text{B.15})$$

In case of axion production from decays, the same steps yield for the collision term

$$\begin{aligned} \mathcal{C}_{p_1 \rightarrow p_2 a} &= \int d\Pi_1 d\Pi_2 d\Pi_a f_1^{\text{eq}} (2\pi)^4 \delta^4(p_1 - p_2 - p_a) |\mathcal{M}_{p_1 \rightarrow p_2 a}|^2 \\ &= g_1 \Gamma_{p_1 \rightarrow p_2 a} \int \frac{d^3 p}{(2\pi)^3} \frac{m_1}{E_1} f_1^{\text{eq}} \\ &= n_1^{\text{eq}} \Gamma_{p_1 \rightarrow p_2 a} \frac{K_1(m_1/T)}{K_2(m_1/T)}, \end{aligned} \quad (\text{B.16})$$

where $|\mathcal{M}_{p_1 \rightarrow p_2 a}|^2$ is the squared matrix element of the decay process including sums over initial and final polarizations (no averaging), and $\Gamma_{p_1 \rightarrow p_2 a}$ denotes the decay rate in the rest frame of particle 1, given by

$$\Gamma_{p_1 \rightarrow p_2 a} = \frac{1}{16\pi g_1 m_1} |\mathcal{M}_{p_1 \rightarrow p_2 a}|^2 \lambda^{1/2} \left(\frac{m_2}{m_1}, \frac{m_a}{m_1} \right). \quad (\text{B.17})$$

If the mass of the axion is neglected, this simplifies to

$$\Gamma_{p_1 \rightarrow p_2 a} = \frac{1}{16\pi g_1 m_1} |\mathcal{M}_{p_1 \rightarrow p_2 a}|^2 \left(1 - \frac{m_2^2}{m_1^2}\right). \quad (\text{B.18})$$

The axion production rate from decays is finally given by

$$\Gamma_{p_1 \rightarrow p_2 a}(T) = \frac{n_1^{\text{eq}}}{n_a^{\text{eq}}} \Gamma_{p_1 \rightarrow p_2 a} \frac{K_1(m_1/T)}{K_2(m_1/T)}, \quad (\text{B.19})$$

and for the total production rate from decays all processes have to be summed

$$\Gamma_D(T) = \sum_{p_1} \Gamma_{p_1 \rightarrow p_2 a}(T), \quad (\text{B.20})$$

including charge multiplicities, e.g. for a single charged lepton $p_1 = \ell^+, \ell^-$.

B.3 Pion and Kaon Scatterings

Scattering with pions is usually the main channel of axion production. Given the coupling Eq. (A.11), the known amplitude for three processes $\pi^0\pi^\pm \rightarrow a\pi^\pm$, $\pi^+\pi^- \rightarrow a\pi^0$ evaluates to [79]

$$\sum_{\text{processes}} |\mathcal{M}|_{\pi\pi \rightarrow a\pi}^2 = \frac{9}{4} \left(\frac{C_\pi}{f_\pi f_a} \right)^2 (s^2 + t^2 + u^2 - 3m_\pi^4). \quad (\text{B.21})$$

Neglecting the mass splitting between charged and neutral pions, we obtain a total thermally averaged cross section for all three processes using Eq. (B.11) and Eq.(B.14). However, because ChPT is only EFT the integral in Eq. (B.11) should only be performed up to cut-off $\sqrt{s} = \Lambda_{\text{ChPT}} = 4\pi f_\pi$. Otherwise, artificial contributions from divergent cross section would alter high-temperature behaviour of scattering rate.

Since pions are present in the thermal bath only after the QCDPT, we include this contribution in Boltzmann equation only for $T < T_{\text{QCD}} = 158 \text{ MeV}$ [80] by adding the Heaviside theta function $\theta(T_{\text{QCD}} - T)$. It is worth mentioning that working in LO of ChPT has been shown to be unreliable at temperature above $T \simeq 70 \text{ MeV}$ [81, 82]. This contribution has been recently calculated precisely using phenomenological cross section [16]. However, the LO ChPT suffices to show that in models considered in this work, pions give negligible contribution to the ΔN_{eff} .

The scattering rate for processes involving kaons and pions $\pi K \rightarrow Ka$ have been calculated in case of hadronic axions [16]. In nucleophobic models these scattering rates are suppressed unless $C_s \neq 0$, as explained above Eq. (A.14). Given interactions Eq. (A.13) we used FeynRules [83] and FeynCalc [84, 85] to derive the scattering amplitude for 8 processes: $\pi^0 K^\pm, K^0 \pi^\pm \rightarrow a\pi^\pm$; $\pi^0 K^0, \pi^- K^+ \rightarrow aK^0$; $\pi^+ K^-, \pi^0 \bar{K}^0 \rightarrow a\bar{K}^0$, which for $w = 0, z = 1/2$ is given by a simple formula

$$\sum_{\text{processes}} |\mathcal{M}|_{\pi K \rightarrow aK}^2 = \left(\frac{\sqrt{3}C_s}{2f_\pi f_a} \right)^2 t^2. \quad (\text{B.22})$$

We neglect the mass splitting of kaons, and pions using formulas Eq. (B.11) and Eq. (B.14) to obtain the rates. We take into account production from those scatterings below the QCDPT by adding the Heaviside theta function to the rate. The suppression of this rate with respect to the pion scatterings rate comes mostly from the Boltzmann factors.

Since LO of ChPT breaks down around $T \sim 70 \text{ MeV}$, our results should be taken with a grain of salt. The calculation of the scatterings rate in NLO ChPT is beyond the scope of this paper, and we leave it for future work.

B.4 Lepton flavor-conserving Scatterings

There are two leptonic processes that thermalize axions and conserve flavor - lepton annihilation $\ell^+\ell^- \rightarrow \gamma a$ and Compton-like scattering with axions at the final state $\ell^\pm \gamma \rightarrow \ell^\pm a$. The resulting production rates are well-known, and for completeness we quote the results.

Two tree-level diagrams, u - and t -channel, contribute to process $\ell^+\ell^- \rightarrow \gamma a$. Upon phase space integration, the cross section as a function of center of mass energy is given

by [55]

$$\sigma_{\ell^+\ell^-\rightarrow\gamma a}(s) = \frac{e^2 C_\ell^2 m_\ell^2}{4\pi f_a^2 (s - 4m_\ell^2)} \tanh^{-1} \left(\sqrt{1 - \frac{4m_\ell^2}{s}} \right). \quad (\text{B.23})$$

Two diagrams (s - and u -channel) contribute to the cross section for Compton-like scattering $\ell^\pm\gamma \rightarrow \ell^\pm a$, which reads [55]

$$\sigma_{\ell^\pm\gamma\rightarrow\ell^\pm a}(s) = \frac{C_\ell^2 m_\ell^2 e^2}{32\pi f_a^2} \frac{2s^2 \log(s/m_\ell^2) - 3s^2 + 4m_\ell^2 s - m_\ell^4}{s^2 (s - m_\ell^2)}. \quad (\text{B.24})$$

For large s both scattering processes have the same scaling $\sigma \sim m_\ell^2/f_a^2 \log s/s$. This gives the scaling of the thermally averaged cross-sections in Eq. (B.12) for large T as

$$\langle\sigma v\rangle_{\ell^+\ell^-\rightarrow\gamma a} \xrightarrow{T \gg m_\ell} \frac{C_\ell^2 m_\ell^2 e^2}{32\pi f_a^2 T^2} \log \frac{2T}{m_\ell}, \quad (\text{B.25})$$

$$\langle\sigma v\rangle_{\ell^\pm\gamma\rightarrow\ell^\pm a} \xrightarrow{T \gg m_\ell} \frac{C_\ell^2 m_\ell^2 e^2}{64\pi f_a^2 T^2} \log \frac{2T}{m_\ell}, \quad (\text{B.26})$$

so that the production rates at high temperatures are

$$\Gamma_{\ell^+\ell^-\rightarrow\gamma a}(T) \xrightarrow{T \gg m_\ell} \frac{C_\ell^2 m_\ell^2 e^2 T}{8\pi^3 \zeta(3) f_a^2} \log \frac{2T}{m_\ell}, \quad (\text{B.27})$$

$$\Gamma_{\ell^\pm\gamma\rightarrow\ell^\pm a}(T) \xrightarrow{T \gg m_\ell} \frac{C_\ell^2 m_\ell^2 e^2 T}{16\pi^3 \zeta(3) f_a^2} \log \frac{2T}{m_\ell}. \quad (\text{B.28})$$

The total axion production rate from scatterings at high temperatures is then given by

$$\begin{aligned} \Gamma_S(T) &= \Gamma_{\ell^+\ell^-\rightarrow\gamma a}(T) + \Gamma_{\ell^+\gamma\rightarrow\ell^+ a}(T) + \Gamma_{\ell^-\gamma\rightarrow\ell^- a}(T) \\ &\xrightarrow{T \gg m_\ell} \frac{C_\ell^2 \alpha m_\ell^2 T}{\pi^2 \zeta(3) f_a^2} \log \frac{2T}{m_\ell}. \end{aligned} \quad (\text{B.29})$$

In the freeze-in regime axion production is dominated by temperatures slightly below m_ℓ , and we approximate the scattering rate in this regime simply by taking the high-temperature expression above without the log but with a Boltzmann suppression factor, i.e.

$$\Gamma_S(T) \xrightarrow{T \lesssim m_\ell} \frac{C_\ell^2 \alpha m_\ell^2 T}{\pi^2 \zeta(3) f_a^2} e^{-\frac{m_\ell}{T}}. \quad (\text{B.30})$$

Instead for very low temperatures the scaling of the two processes with T is different

$$\langle\sigma v\rangle_{\ell^+\ell^-\rightarrow\gamma a} \xrightarrow{T \ll m_\ell} \frac{C_\ell^2 e^2}{8\pi f_a^2}, \quad (\text{B.31})$$

$$\langle\sigma v\rangle_{\ell^\pm\gamma\rightarrow\ell^\pm a} \xrightarrow{T \ll m_\ell} \frac{C_\ell^2 e^2 T^2}{\pi m_\ell^2 f_a^2}, \quad (\text{B.32})$$

and the production rates at low temperatures are Boltzmann suppressed

$$\Gamma_{\ell^+\ell^-\rightarrow\gamma a}(T) \xrightarrow{T \ll m_\ell} \frac{C_\ell^2 e^2 m_\ell^3}{16\pi^2 \zeta(3) f_a^2} e^{-\frac{2m_\ell}{T}}, \quad (\text{B.33})$$

$$\Gamma_{\ell^\pm\gamma\rightarrow\ell^\pm a}(T) \xrightarrow{T \ll m_\ell} \sqrt{\frac{2T}{\pi m_\ell}} \frac{C_\ell^2 e^2 T^3}{\pi^2 \zeta(3) f_a^2} e^{-\frac{m_\ell}{T}}. \quad (\text{B.34})$$

B.5 Lepton flavor-violating Decays

The decay rate for the process $\ell \rightarrow \ell' a$ is given by [55]

$$\Gamma_{\ell^\pm \rightarrow \ell'^\pm a} = C_{\ell\ell'}^2 \frac{m_\ell^3}{64\pi f_a^2} \left(1 - \frac{m_{\ell'}^2}{m_\ell^2}\right)^3 \approx C_{\ell\ell'}^2 \frac{m_\ell^3}{64\pi f_a^2}, \quad (\text{B.35})$$

where the last approximation holds to good approximation as lepton masses are strongly hierarchical. The axion production rate from decays can be computed using Eq. (B.20), which gives⁹

$$\Gamma_D(T) = \frac{g_1}{2\pi^2} m_\ell^2 T K_1(m_\ell/T) (\Gamma_{\ell^+ \rightarrow \ell'^+ a} + \Gamma_{\ell^- \rightarrow \ell'^- a}), \quad (\text{B.36})$$

with $g_1 = 2$ for spin degrees of freedom. For large temperatures this becomes

$$\Gamma_D(T) \xrightarrow{T \gg m_\ell} \frac{C_{\ell\ell'}^2 m_\ell^4}{32\pi\zeta(3)f_a^2 T}, \quad (\text{B.37})$$

When T drops below the lepton mass m_ℓ , the production rate becomes Boltzmann suppressed, giving

$$\Gamma_D(T) \xrightarrow{T \lesssim m_\ell} \frac{C_{\ell\ell'}^2 m_\ell^4}{32\pi\zeta(3)f_a^2 T} e^{-\frac{m_\ell}{T}}, \quad (\text{B.38})$$

while for very low temperatures one obtains

$$\Gamma_D(T) \xrightarrow{T \ll m_\ell} \sqrt{\frac{2T}{\pi m_\ell}} \frac{C_{\ell\ell'}^2 m_\ell^5}{64\zeta(3)f_a^2 T^2} e^{-\frac{m_\ell}{T}}. \quad (\text{B.39})$$

C Boltzmann Equation

The number density n_a of axions is governed by the integrated Boltzmann equation [87]

$$\frac{dn_a}{dt} + 3Hn_a = \left(\sum_i \Gamma_i\right) \left(n_a^{\text{eq}} - n_a\right), \quad (\text{C.1})$$

where n_a^{eq} is the number density of axions at equilibrium, H is the Hubble parameter

$$H = \frac{T^2}{M_{\text{Pl}}} 1.66 \sqrt{g_*(T)}, \quad (\text{C.2})$$

with $g_*(T)$ denoting the total number of relativistic degrees of freedom and Γ_i are the single axion production rates considered above. It is convenient to work with dimensionless temperature variables $x = m/T$ and the yields $Y_a = n_a/s$, where m is chosen as the mass of

⁹Flavor-violating scatterings $\ell\gamma \rightarrow \ell'a$ and $\ell\ell' \rightarrow \gamma a$ have infrared divergence, which should cancel against real and virtual corrections to the tree-level decay rate. This has been demonstrated for the case of $\ell\gamma \rightarrow \ell'a$ in Ref. [86], and we expect a similar behaviour for $\ell\ell' \rightarrow \gamma a$, at least for small $T \lesssim m_\ell$. Therefore these processes should only give sub-leading contribution to the axion production rate (peaked at $T \lesssim m_\ell/3$) and thus are omitted here.

the heaviest particle involved in the production process (in our calculations we use $m = m_\tau$) and s is the entropy density

$$s = \frac{2\pi^2 T^3}{45} g_{*s}(T), \quad (\text{C.3})$$

where $g_{*s}(T)$ is the effective number of relativistic entropy degrees of freedom¹⁰ It is clear that Y_a^{eq} remains constant as long as g_{*s} does not change. Since axions decouple around the QCDPT, there is a rapid change in g_{*s} , and accordingly the equilibrium yield changes as well.

Using entropy conservation, $d(sa^3)/dt = 0$, we can express the time-derivative as

$$\frac{dx}{dt} = xH \left(\frac{T}{3s} \frac{ds}{dT} \right)^{-1} = xH \left(1 - \frac{x}{3g_{*s}} \frac{dg_{*s}}{dx} \right)^{-1}. \quad (\text{C.4})$$

The Boltzmann equation in new variables reads

$$sHx \frac{dY_a}{dx} = \left(1 - \frac{x}{3g_{*s}} \frac{dg_{*s}}{dx} \right) n_a^{\text{eq}} \sum_i \Gamma_i \left(1 - \frac{Y_a}{Y_a^{\text{eq}}} \right). \quad (\text{C.5})$$

We solve this equation numerically on the interval $x \in [0.01, 190]$ assuming vanishing initial yield, $Y_a^i = Y_a(x=0.01) = 0$. Note that axion production from electron scattering is active at $T \sim m_e$, in this case we solve the Boltzmann equation up to $x = 4000$. In order to improve the computation time, we evaluate the rates Γ_i for logarithmically distributed points x_i and use the spline interpolation to recover continuous functions.

Thermal axions contribute to the total energy density of radiation, which is parametrized by the additional effective number of neutrinos ΔN_{eff} as

$$\Delta N_{\text{eff}} = \frac{8}{7} \left(\frac{11}{4} \right)^{\frac{4}{3}} \frac{\rho_a}{\rho_\gamma} \Big|_{T_{\text{CMB}}}, \quad (\text{C.6})$$

where ρ_γ and ρ_a are the energy densities of photons and axions, respectively. One can estimate ρ_a in terms of the axion number density n_a , and ρ_γ in terms of the entropy density s , obtaining [17]

$$\Delta N_{\text{eff}} = \frac{4}{7} \left(\frac{11}{4} \right)^{\frac{4}{3}} \left(\frac{2\pi^4}{45\zeta(3)} g_{*s}(T_{\text{CMB}}) Y_a(T_{\text{CMB}}) \right)^{\frac{4}{3}}. \quad (\text{C.7})$$

Although ΔN_{eff} is set by the axion yield at T_{CMB} , we may identify it with the asymptotic yield $Y_a|_{T_{\text{CMB}}} = Y_a^\infty$, which we numerically evaluate at the endpoint of the Boltzmann integration interval since at late times all axion interactions are frozen. If the yield of axions is small we can simply take $g_{*s}(T_{\text{CMB}}) \simeq g_{*s}^{\text{SM}}(T_{\text{CMB}}) = 43/11$ and the numerical formula reads

$$\Delta N_{\text{eff}} = 74.85 (Y_a^\infty)^{\frac{4}{3}}. \quad (\text{C.8})$$

¹⁰We use the results from Ref. [88] for both $g_{*s}(T)$ and $g_*(T)$, but our results are not very sensitive on the exact values of g_* we use, which has already been noted in Ref. [55].

However, if the abundance of axions is large, we cannot neglect their contribution to the number of entropic degrees of freedom and a better estimate reads [17]

$$\Delta N_{\text{eff}} = \frac{4}{7} \left(\frac{11}{4} \right)^{\frac{4}{3}} \left(\frac{\frac{2\pi^4}{45\zeta(3)} g_{*s}^{\text{SM}}(T_{\text{CMB}}) Y_a^\infty}{1 - \frac{2\pi^4}{45\zeta(3)} Y_a^\infty} \right)^{\frac{4}{3}}. \quad (\text{C.9})$$

We use this expression throughout our analysis, although its effect is non-negligible only for $\Delta N_{\text{eff}} \gtrsim 0.2$, and even then is merely a few-percent correction compared to Eq. (C.8).

We note that the estimate in Eq. (C.9) gives a good approximation only when the axion follows a thermal distribution, which is the case for freeze-out production. Instead for freeze-in production Eq. (C.9) underestimates ΔN_{eff} . This is because Eq. (C.7) is based on the assumption that $\rho_a = \pi^2(\pi^2 n_a / \zeta(3))^{4/3} / 30$, for which the typical energy of axions is $\rho_a / n_a \sim n_a^{1/3}$. However, for freeze-in production $n_a^{1/3}$ is smaller than the actual typical energy $(n_a^{\text{eq}})^{1/3} \sim T$ of thermally produced axions, so that the actual energy density of the axions is larger than obtained from Eq. (C.7).

Let us estimate how much we underestimate ΔN_{eff} . A more precise estimate of ρ_a is

$$\rho_{a,1} = \rho_a^{\text{eq}} \frac{n_a}{n_a^{\text{eq}}} \quad (\text{C.10})$$

at the temperature T_{FI} where the freeze-in production is peaked at. This relation is justified since typically $\dot{\rho}_a / \rho_a^{\text{eq}} \simeq \dot{n}_a / n_a^{\text{eq}}$. Taking the ratio with the energy density $\rho_{a,2}$ estimated by $\rho_{a,2} = \pi^2(\pi^2 n_a / \zeta(3))^{4/3} / 30$, we obtain

$$\frac{\rho_{a,2}}{\rho_{a,1}} \simeq 0.5 \left(\frac{\Delta N_{\text{eff}}}{0.05} \right)^{1/4} \left(\frac{g_{*s}(T_{\text{FI}})}{10} \right)^{1/3}, \quad (\text{C.11})$$

where ΔN_{eff} is obtained by Eq. (C.8). One can see that the underestimation is more significant when ΔN_{eff} is smaller and the freeze-in production is peaked at lower temperatures. The most underestimated channel is the scattering off muons, where $g_{*s}(T_{\text{FI}}) \simeq 10$. For the phenomenologically interesting range $\Delta N_{\text{eff}} > 0.05$, the underestimation is at most off by a factor 2. This corresponds only to a 30% change in f_a since $\Delta N_{\text{eff}} \propto f_a^{-8/3}$. For freeze-in production by other particles, where $g_{*s}(T_{\text{FI}})$ is larger, the impact is even smaller.

Given that ΔN_{eff} is appreciably underestimated only for the production off muons, we use Eq. (C.9) throughout the paper. Note that Eq. (C.10) is also still approximate and requires the determination of T_{FI} . A more exact computation will require the derivation of $\dot{\rho}_a$, which we leave for future work.

C.1 Approximate Solution to Boltzmann Equation

It is possible to obtain an approximate analytic solution of the Boltzmann equation if one assumes approximately constant g_{*s} [23, 55], which allows to simplify $g'_{*s}(x) = 0$ and take Y_a^{eq} constant. Re-introducing the collision operators $\mathcal{C}_i = n_a^{\text{eq}} \Gamma_i$ with i denoting collectively scattering and decays, the Boltzmann equation (C.5) simplifies to

$$\frac{dY_a}{1 - \frac{Y_a}{Y_a^{\text{eq}}}} = \frac{\sum_i \mathcal{C}_i(x) x^4 dx}{H(m) s(m)}, \quad (\text{C.12})$$

where we used the temperature scaling of entropy density and Hubble rate scale $H(x) = H(m)x^{-2}$, $s(x) = s(m)x^{-3}$ for constant g_{*s} . With the initial condition $Y(x=0) = 0$ one can integrate both sides to obtain the late-time yield $Y_a^\infty = Y_a(x \rightarrow \infty)$ as

$$Y_a^\infty = Y_a^{\text{eq}}(m) \left(1 - \exp \left[- \frac{\sum_i \int_0^\infty x^4 \mathcal{C}_i(x) dx}{H(m)s(m)Y_a^{\text{eq}}(m)} \right] \right). \quad (\text{C.13})$$

where we have evaluated for definiteness Y_a^{eq} at $T = m$. We now perform the remaining integral using the exact expressions in Eq. (B.8) and (B.16). The latter gives (adding a factor 2 for charge multiplicities)

$$\mathcal{C}_{p_1 \rightarrow p_2 a}(x) = C_{\ell\ell'}^2 \frac{m_\ell^6}{32\pi^3 f_a^2} \frac{K_1(x)}{x}, \quad (\text{C.14})$$

and since

$$\int_0^\infty x^3 K_1(x) dx = \frac{3\pi}{2}, \quad (\text{C.15})$$

we obtain for decays

$$\int_0^\infty x^4 \mathcal{C}_{p_1 \rightarrow p_2 a}(x) = C_{\ell\ell'}^2 \frac{3m_\ell^6}{64\pi^2 f_a^2}. \quad (\text{C.16})$$

Instead for scattering the collision operators are (including a factor of 2 for charge multiplicity in $\ell^\pm \gamma \rightarrow \ell^\pm a$)

$$\begin{aligned} \mathcal{C}_{\ell^+ \ell^- \rightarrow \gamma a}(x) &= \frac{m_\ell}{8\pi^4 x} \int_{4m_\ell^2}^\infty \left(1 - \frac{4m_\ell^2}{s} \right) s^{3/2} \sigma_{\ell^+ \ell^- \rightarrow \gamma a}(s) K_1 \left(\frac{x\sqrt{s}}{m_\ell} \right) ds, \\ &= \frac{4m_\ell^6}{\pi^4 x} \int_0^\infty y \sqrt{1+y} \sigma_{\ell^+ \ell^- \rightarrow \gamma a}(y) K_1 \left(2x\sqrt{1+y} \right) dy, \end{aligned} \quad (\text{C.17})$$

where we substituted $s = 4m_\ell^2(1+y)$, and

$$\begin{aligned} \mathcal{C}_{\ell^\pm \gamma \rightarrow \ell^\pm a}(x) &= \frac{m_\ell}{4\pi^4 x} \int_{m_\ell^2}^\infty \left(1 - \frac{m_\ell^2}{s} \right)^2 s^{3/2} \sigma_{\ell^\pm \gamma \rightarrow \ell^\pm a}(s) K_1 \left(\frac{x\sqrt{s}}{m_\ell} \right) ds, \\ &= \frac{m_\ell^6}{4\pi^4 x} \int_0^\infty \frac{y^2}{\sqrt{1+y}} \sigma_{\ell^\pm \gamma \rightarrow \ell^\pm a}(y) K_1 \left(x\sqrt{1+y} \right) dy, \end{aligned} \quad (\text{C.18})$$

where we substituted $s = m_\ell^2(1+y)$. While these integrals are difficult, we can perform first the temperature (i.e. x) integration of the integrand, which leaves an expression that can be easily integrated over y analytically, giving in total for scattering

$$\int_0^\infty x^4 \mathcal{C}_{p_1 p_2 \rightarrow p_3 a}(x) = C_{\ell\ell}^2 \frac{\alpha m_\ell^6}{\pi^2 f_a^2} \begin{cases} \frac{3}{32} & \ell^+ \ell^- \rightarrow \gamma a \\ \frac{4}{21\pi} & \ell^\pm \gamma \rightarrow \ell^\pm a \end{cases}. \quad (\text{C.19})$$

C.2 Thermal Freeze-Out

If interactions bring axions into thermal equilibrium at early times, i.e. $\Gamma_i(m)/H(m) \gg 1$, which can always be achieved for sufficiently small f_a , the late-time abundance is dominated by the first term in Eq. (C.13). This gives the yield as $Y_a^\infty = Y_a^{\text{eq}}(T_d)$, where T_d is the decoupling temperature defined by $H(T_d) = \Gamma_i(T_d)$, which enters the yield only through $g_{*s}(T_d)$. The latter decreases with f_a , so for sufficiently small f_a the late-time yield reaches a plateau, and so does ΔN_{eff} according to Eq. (C.8), or better (C.9).

We now estimate the decoupling temperature and the corresponding yield using the asymptotic forms of the scattering and decay rates. Since decoupling happens at moderately late times $x \approx m/10$, we use the asymptotic forms in the low-temperature regime Eq. (B.30) and Eq. (B.38). The decoupling temperatures for scattering and decays are thus given by solving

$$T_S^d \approx m \log \left[\frac{C^2 \alpha m^2 M_{\text{Pl}}}{1.66 \sqrt{g_{*s}(T_S^d)} \pi^2 \zeta(3) f_a^2 T_S^d} \right], \quad (\text{C.20})$$

$$T_D^d \approx m \log \left[\frac{C^2 m^4 M_{\text{Pl}}}{1.66 \sqrt{g_{*s}(T_D^d)} 32 \pi \zeta(3) f_a^2 (T_D^d)^3} \right]. \quad (\text{C.21})$$

C.3 Thermal Freeze-In

When the interactions are too weak to bring axions to equilibrium, $\Gamma_i(m)/H(m) \ll 1$, which happens for sufficiently large f_a , one can expand the exponential in Eq. (C.13) to leading order obtaining

$$Y_a^\infty \simeq Y_a^{\text{eq}}(m) \frac{\sum_i \int_0^\infty x^4 \mathcal{C}_i(x) dx}{H(m) s(m) Y_a^{\text{eq}}(m)} = \frac{m_\ell^6}{\pi^2 f_a^2 H(m) s(m)} \begin{cases} C_{\ell\ell}^2 \frac{3\alpha}{32} & \ell^+ \ell^- \rightarrow \gamma a \\ C_{\ell\ell}^2 \frac{4\alpha}{21\pi} & \ell^\pm \gamma \rightarrow \ell^\pm a \\ C_{\ell\ell'}^2 \frac{3}{64} & \ell^\pm \rightarrow \ell'^\pm a \end{cases}$$

$$= 1.4 \times 10^{-3} \frac{m_\ell M_{\text{Pl}}}{f_a^2 g_{*s}(m_\ell) \sqrt{g_*(m_\ell)}} \begin{cases} 9.4\alpha C_{\ell\ell}^2 & \ell^+ \ell^- \rightarrow \gamma a \\ 6.1\alpha C_{\ell\ell}^2 & \ell^\pm \gamma \rightarrow \ell^\pm a \\ 4.7 C_{\ell\ell'}^2 & \ell^\pm \rightarrow \ell'^\pm a \end{cases}, \quad (\text{C.22})$$

so apart from the α -suppression scattering and decays give similar contributions (see also Ref. [89, 90]). The yields scale as m_ℓ/f_a^2 , so that one obtains with Eq. (C.8) the scaling $\Delta N_{\text{eff}} \propto f_a^{-8/3}$. These analytic formulas agree quite well with the numerical results (less so for muon scattering and decays, since the number of SM relativistic degrees of freedom changes rapidly around the muon mass).

C.4 Transition Region

We now estimate the temperature T^{eq} at which scatterings or decays bring axions into thermal equilibrium in the very early universe at $T \gg m$, which happens only for sufficiently

	q_{L3}	q_{La}	u_{R3}	u_{Ra}	d_{R3}	d_{Ra}	ℓ_{L3}	ℓ_{La}	e_{R3}	e_{Ra}	h_i	ϕ
$U(1)_{\text{PQ}}$	X_{q_3}	X_{q_a}	X_{u_3}	X_{u_a}	X_{d_3}	X_{d_a}	X_{ℓ_3}	X_{ℓ_a}	X_{e_3}	X_{e_a}	X_i	X_ϕ

Table D1. PQ charge assignments, $a = 1, 2$ denotes the first two fermion generations, while $i = 0, \dots, n - 1$ runs over Higgs doublets.

small f_a . For this we evaluate the defining equations $H(T_i^{\text{eq}}) = \Gamma_i(T_i^{\text{eq}})$ in the high-temperature regime for the rates, using Eq. (B.29) and (B.37). This leads to

$$T_S^{\text{eq}} \approx \frac{C_{\ell\ell}^2 \alpha m_\ell^2 M_{\text{Pl}}}{\pi^2 1.66 \zeta(3) \sqrt{g_{*s}^{\text{UV}}} f_a^2} \log \frac{2C_{\ell\ell}^2 \alpha m_\ell M_{\text{Pl}}}{\pi^2 1.66 \zeta(3) \sqrt{g_{*s}^{\text{UV}}} f_a^2}, \quad (\text{C.23})$$

$$T_D^{\text{eq}} \approx \left(\frac{C_{\ell\ell'}^2 m_\ell^4 M_{\text{Pl}}}{32\pi 1.66 \zeta(3) \sqrt{g_{*s}^{\text{UV}}} f_a^2} \right)^{1/3}, \quad (\text{C.24})$$

where we worked at logarithmic accuracy in T_S^{eq} and approximated in both cases $g_{*s}(T_i^{\text{eq}}) \approx g_{*s}^{\text{UV}} \approx 104$, since $T_i^{\text{eq}} \gg \text{TeV}$. The point $T_i^{\text{eq}} \approx m_\ell$ marks the transition regime between freeze-out and freeze-in, which we can estimate extrapolating the high-temperature expressions above. It corresponds to the axion decay constant $(f_a/C_i)_i^{\text{eq}}$ given by

$$\begin{aligned} (f_a/C_{\ell\ell})_S^{\text{eq}} &\approx \left(\frac{\alpha m_\ell M_{\text{Pl}}}{\pi^2 1.66 \zeta(3) \sqrt{g_{*s}^{\text{UV}}} \log 2} \right)^{1/2} = 2 \times 10^7 \text{ GeV} \sqrt{\frac{m_\ell}{\text{GeV}}}, \\ (f_a/C_{\ell\ell'})_D^{\text{eq}} &\approx \left(\frac{m_\ell M_{\text{Pl}}}{32\pi 1.66 \zeta(3) \sqrt{g_{*s}^{\text{UV}}}} \right)^{1/2} = 8 \times 10^7 \text{ GeV} \sqrt{\frac{m_\ell}{\text{GeV}}}. \end{aligned} \quad (\text{C.25})$$

D Astrophobic DFSZ Models

In this appendix we describe in detail the construction of astrophobic DFSZ models as SM extensions with two or three Higgs doublets. We begin with the general description of the quark Yukawa sector and the resulting axion couplings, which are determined by the PQ charges of Higgs doublets and flavor rotations. The form of the scalar potential then fixes all charges in terms of the discrete choices for the Yukawa sector, the vacuum angles and flavor rotations. By scanning over these possibilities, we systematically identify all nucleophobic models, for models with two and three Higgs doublets. We finally include the charged lepton Yukawa sector and construct models with suppressed couplings to electrons, muons and/or photons.

D.1 Quark Yukawa Sector

To the SM fermion fields we add n scalar Higgs doublets h_i with hypercharge $Y = -1/2$ and a complex singlet scalar ϕ . The quark Lagrangian is taken to be invariant under a $U(1)_{\text{PQ}}$ symmetry, with the most general charge assignment consistent with a $2 + 1$ flavor structure, as shown in Table D1. The general quark Yukawa Lagrangian reads

$$\mathcal{L} = -y_{33}^u \bar{q}_{L3} u_{R3} h_{33}^u - y_{3a}^u \bar{q}_{L3} u_{Ra} h_{3a}^u - y_{a3}^u \bar{q}_{La} u_{R3} h_{a3}^u - y_{ab}^u \bar{q}_{La} u_{Rb} h_{ab}^u$$

$$+ y_{33}^d \bar{q}_{L3} d_{R3} \tilde{h}_{33}^d + y_{3a}^d \bar{q}_{L3} d_{Ra} \tilde{h}_{3a}^d + y_{a3}^d \bar{q}_{La} d_{R3} \tilde{h}_{a3}^d + y_{ab}^d \bar{q}_{La} d_{Rb} \tilde{h}_{ab}^d + \text{h.c.}, \quad (\text{D.1})$$

where $\tilde{h}_i = i\sigma^2 h_i^*$, $a, b = 1, 2$ and each Higgs is chosen from the set of n Higgs fields h_i , $i = 0 \dots n-1$, e.g., $h_{3a}^u = h_2, h_{33}^d = h_0$, etc. Schematically, one has

$$y_u \sim \begin{pmatrix} h_{ab}^u & h_{a3}^u \\ h_{3a}^u & h_{33}^u \end{pmatrix}, \quad y_d \sim \begin{pmatrix} h_{ab}^d & h_{a3}^d \\ h_{3a}^d & h_{33}^d \end{pmatrix}, \quad (\text{D.2})$$

where we indicate in $\mathbf{2} + \mathbf{1}$ flavor space to which Higgs field the respective quark bilinears couple to. Note that we require that all Yukawa couplings are allowed by the PQ symmetry, i.e., there are no Yukawa textures (for models where this assumption is relaxed see e.g., Ref. [29]). This gives five constraints, which determines fermion charges in terms of Higgs charges, up to a single quark charge X_{q3} ¹¹

$$X_{u_a} = -X_{h_{3a}^u} + X_{q3}, \quad X_{d_a} = X_{h_{3a}^d} + X_{q3}, \quad X_{q_a} = -X_{h_{33}^u} + X_{h_{a3}^u} + X_{q3} \quad (\text{D.3})$$

$$X_{u_3} = -X_{h_{33}^u} + X_{q3}, \quad X_{d_3} = X_{h_{33}^d} + X_{q3}. \quad (\text{D.4})$$

Moreover, there are three consistency conditions relating Higgs charges as

$$X_{h_{33}^u} - X_{h_{a3}^u} = X_{h_{3a}^u} - X_{h_{ab}^u} = X_{h_{a3}^d} - X_{h_{33}^d} = X_{h_{ab}^d} - X_{h_{3a}^d}. \quad (\text{D.5})$$

D.2 Axion Couplings

The scalar potential is constructed with a single global $U(1)_{\text{PQ}}$ symmetry, and suitable to generate vacuum expectation values for ϕ and all Higgs doublets h_i . The vacuum configuration breaks the global PQ symmetry spontaneously, and the corresponding Goldstone boson is the axion, which enters the Lagrangian as the phase of ϕ and Higgs fields. Since Yukawas are PQ invariant, the axion couplings can be removed by performing the following flavor-diagonal fermion field redefinitions (which is just a local PQ transformation acting only on fermions)

$$f \rightarrow f e^{iX_f a(x)/v_{\text{PQ}}}. \quad (\text{D.6})$$

Since this transformation is anomalous, it generates axion couplings to gauge field strengths, and since it is local it modifies the fermion kinetic terms. Here v_{PQ} denotes the PQ breaking scale, which for $v_\phi \gg v_i$ is set by the singlet vev, $v_{\text{PQ}} \approx X_\phi v_\phi$.

The axion couplings to gluons and photons are given by

$$\mathcal{L}_{\text{anom}} = N \frac{a}{v_{\text{PQ}}} \frac{\alpha_s}{4\pi} G_{\mu\nu} \tilde{G}^{\mu\nu} + E \frac{a}{v_{\text{PQ}}} \frac{\alpha_{\text{em}}}{4\pi} F_{\mu\nu} \tilde{F}^{\mu\nu}, \quad (\text{D.7})$$

with the dual field strength $\tilde{F}_{\mu\nu} = \frac{1}{2} \xi_{\mu\nu\rho\sigma} F^{\rho\sigma}$, $\xi^{0123} = -1$ and the anomaly coefficients

$$\begin{aligned} 2N &= 4X_{q_a} - X_{u_3} - 2X_{u_a} - X_{d_3} - 2X_{d_a} \\ &= 2X_{h_{ab}^u} + X_{h_{33}^u} - 2X_{h_{ab}^d} - X_{h_{33}^d}, \end{aligned} \quad (\text{D.8})$$

¹¹This follows from conserved baryon number, which could be used to redefine $U(1)_{\text{PQ}}$ such that $X_{q3} = 0$.

$$\begin{aligned}
E &= E_Q + E_L \\
&= \frac{5}{3}(2X_{q_a} + X_{q_3}) - \frac{4}{3}(2X_{u_a} + X_{u_3}) - \frac{1}{3}(2X_d + X_{d_3}) + E_L \\
&= \frac{8}{3}X_{h_{ab}^u} + \frac{4}{3}X_{h_{33}^u} - \frac{2}{3}X_{h_{ab}^d} - \frac{1}{3}X_{h_{33}^d} + E_L,
\end{aligned} \tag{D.9}$$

where we included also a generic contribution from the charged lepton sector E_L , to be discussed below.

From the kinetic terms one obtains axion-fermion couplings in the flavor interaction basis

$$\mathcal{L} = \frac{\partial_\mu a}{v_{\text{PQ}}} \left[\bar{u}_i \gamma^\mu \left(\tilde{C}_{ij}^q P_L + \tilde{C}_{ij}^u P_R \right) u_j + \bar{d}_i \gamma^\mu \left(\tilde{C}_{ij}^q P_L + \tilde{C}_{ij}^d P_R \right) d_j \right], \tag{D.10}$$

with

$$\begin{aligned}
\tilde{C}_{ij}^q &= (X_{h_{33}^u} - X_{h_{a3}^u} - X_{q_3}) \delta_{ij} + \text{diag}(0, 0, X_{h_{a3}^u} - X_{h_{33}^u}), \\
\tilde{C}_{ij}^u &= (X_{h_{3a}^u} - X_{q_3}) \delta_{ij} + \text{diag}(0, 0, X_{h_{33}^u} - X_{h_{3a}^u}), \\
\tilde{C}_{ij}^d &= (-X_{h_{3a}^d} - X_{q_3}) \delta_{ij} + \text{diag}(0, 0, X_{h_{3a}^d} - X_{h_{33}^d}).
\end{aligned} \tag{D.11}$$

In the mass basis we finally obtain

$$\mathcal{L} = \frac{\partial_\mu a}{v_{\text{PQ}}} \bar{u} \gamma^\mu (C^{uL} P_L + C^{uR} P_R) u + \frac{\partial_\mu a}{v_{\text{PQ}}} \bar{d} \gamma^\mu (C^{dL} P_L + C^{dR} P_R) d, \tag{D.12}$$

with

$$\begin{aligned}
C_{ij}^{uL} &= (X_{h_{33}^u} - X_{h_{a3}^u} - X_{q_3}) \delta_{ij} - (X_{h_{33}^u} - X_{h_{a3}^u}) \xi_{ij}^{uL}, \\
C_{ij}^{dL} &= (X_{h_{33}^u} - X_{h_{a3}^u} - X_{q_3}) \delta_{ij} - (X_{h_{33}^u} - X_{h_{a3}^u}) \xi_{ij}^{dL}, \\
C_{ij}^{uR} &= (X_{h_{3a}^u} - X_{q_3}) \delta_{ij} + (X_{h_{33}^u} - X_{h_{3a}^u}) \xi_{ij}^{uR}, \\
C_{ij}^{dR} &= (-X_{h_{3a}^d} - X_{q_3}) \delta_{ij} + (X_{h_{3a}^d} - X_{h_{33}^d}) \xi_{ij}^{dR},
\end{aligned} \tag{D.13}$$

where the flavor structure is controlled by the matrices

$$\xi_{ij}^{fP} \equiv (V_{fP})_{3i}^* (V_{fP})_{3j}, \quad f = u, d, \quad P = L, R, \tag{D.14}$$

which depend on the unitary rotations $(V_{fP})_{ij}$ defined by $(V_{UL})^\dagger m_u V_{UR} = m_u^{\text{diag}}$ etc. They satisfy

$$0 \leq \xi_{ii}^{fP} \leq 1, \quad \sum_i \xi_{ii}^{fP} = 1, \quad |\xi_{ij}^{fP}| = \sqrt{\xi_{ii}^{fP} \xi_{jj}^{fP}}, \tag{D.15}$$

and therefore depend only on 2 independent real parameters in each sector u_L, u_R, d_R .

Finally we adopt the standard convention for the axion decay constant $f_a = v_{\text{PQ}}/(2N)$, and write the Lagrangian as

$$\mathcal{L} = \frac{1}{2}(\partial_\mu a)^2 + \frac{a}{f_a} \frac{\alpha_s}{8\pi} G_{\mu\nu} \tilde{G}^{\mu\nu} + \frac{E}{N} \frac{a}{f_a} \frac{\alpha_{\text{em}}}{8\pi} F_{\mu\nu} \tilde{F}^{\mu\nu} + \frac{\partial_\mu a}{2f_a} \bar{f}_i \gamma^\mu (C_{ij}^V + C_{ij}^A \gamma_5) f_j, \tag{D.16}$$

with

$$C_{u_i u_j}^V = \frac{C_{ij}^{u_R} + C_{ij}^{u_L}}{2N}, \quad C_{u_i u_j}^A = \frac{C_{ij}^{u_R} - C_{ij}^{u_L}}{2N}, \quad (\text{D.17})$$

and analogous for the down-quark coupling.

D.3 Scalar Potential

Compared to the SM the Yukawa Lagrangian has an extra $U(1)_h^n \times U(1)_\phi$ global symmetry that needs to be broken to a single $U(1)_{\text{PQ}}$ factor by adding n couplings in the scalar sector. Since $U(1)_{\text{PQ}} \neq U(1)_\phi$, we need at least one coupling of ϕ . In general we can couple $h_i^\dagger h_j$ to an operator $\mathcal{O}_{ij} \in \{\phi, \phi^*, \phi^2, \phi^{*2}\}$ at the renormalizable level. This determines the charge difference of the Higgs fields in terms of a free parameter A_{ij} that can take the values $A_{ij} \in \{\pm 1, \pm 2\}$. Without loss of generality, we can therefore add suitable couplings in the scalar potential, which determine all Higgs charges in term of a charge X_0 of h_0 and $n - 1$ parameters A_i , which can take discrete values that increase with i

$$X_i = X_0 + A_i X_\phi, \quad A_i = \pm 1, \pm 2, \dots, 2i, \quad i = 0, 1, \dots, n - 1, \quad (\text{D.18})$$

and $A_0 = 0$. Finally the charge X_0 is determined by requiring that the axion is orthogonal to the Goldstone eaten up by the Z -boson, which gives the conditions

$$0 = \sum_i X_i \frac{v_i^2}{v^2}, \quad 1 = \sum_i \frac{v_i^2}{v^2}, \quad (\text{D.19})$$

where the sum is taken over all Higgs fields with vev v_i and $v = 246 \text{ GeV}$ denotes the electroweak vev. This gives

$$X_0 = -X_\phi \sum_i A_i \frac{v_i^2}{v^2}, \quad (\text{D.20})$$

which makes all Higgs charges and thus fermion charges to depend on continuous parameters, that is, the vacuum angles. As the anomaly coefficients are topological in nature, they have to be integers nevertheless, and indeed it is obvious that $2N$ in Eq. (D.8) only depends on Higgs charge differences, so X_0 drops out, and up to an overall charge normalization X_ϕ the color anomaly coefficient is solely determined by A_i . Similarly for the electromagnetic anomaly the charged lepton contribution E_L will provide a complete cancellation of the X_0 dependence, and in the final ratio E/N the charge normalization X_ϕ cancels out leaving a rational number. Also in fermion couplings X_ϕ cancels out, but these couplings depend in general on X_0 . However, the combination $C_{u_i u_j}^A + C_{d_i d_j}^A$ only depends on Higgs charge differences, so again does not depend on vacuum angles.

D.4 Nucleophobic Models

We now restrict for simplicity to at most 3 Higgs doublets. This implies that the consistency conditions

$$X_{h_{33}^u} - X_{h_{a3}^u} = X_{h_{3a}^u} - X_{h_{ab}^u} = X_{h_{a3}^d} - X_{h_{33}^d} = X_{h_{ab}^d} - X_{h_{3a}^d}. \quad (\text{D.21})$$

can only be fulfilled if in each equation Higgses are pairwise identified, giving 2 possibilities for each equation. Counting all distinct possibilities, one finds 7 distinct models, which are

$$\begin{aligned} & \begin{pmatrix} h_b h_b \\ h_a h_a \end{pmatrix} \begin{pmatrix} h_a h_a \\ h_b h_b \end{pmatrix}, \begin{pmatrix} h_a h_a \\ h_a h_a \end{pmatrix} \begin{pmatrix} h_b h_c \\ h_b h_c \end{pmatrix}, \begin{pmatrix} h_b h_a \\ h_b h_a \end{pmatrix} \begin{pmatrix} h_a h_c \\ h_a h_c \end{pmatrix}, \begin{pmatrix} h_b h_a \\ h_b h_a \end{pmatrix} \begin{pmatrix} h_c h_a \\ h_c h_a \end{pmatrix}, \\ & \begin{pmatrix} h_a h_b \\ h_a h_b \end{pmatrix} \begin{pmatrix} h_c h_a \\ h_c h_a \end{pmatrix}, \begin{pmatrix} h_a h_b \\ h_a h_b \end{pmatrix} \begin{pmatrix} h_a h_c \\ h_a h_c \end{pmatrix}, \begin{pmatrix} h_b h_c \\ h_b h_c \end{pmatrix} \begin{pmatrix} h_a h_a \\ h_a h_a \end{pmatrix}. \end{aligned} \quad (\text{D.22})$$

We also restrict to models that potentially have suppressed couplings to nucleons, which mainly depend on the valence quark couplings C_u and C_d , given by

$$C_u \equiv C_u^A = \frac{1}{2N} \left[X_{h_{ab}^u} + (X_{h_{33}^u} - X_{h_{3a}^u}) \xi_{11}^{uR} + (X_{h_{3a}^u} - X_{h_{ab}^u}) \xi_{11}^{uL} \right], \quad (\text{D.23})$$

$$C_d \equiv C_d^A = \frac{1}{2N} \left[-X_{h_{ab}^d} + (X_{h_{3a}^d} - X_{h_{33}^d}) \xi_{11}^{dR} + (X_{h_{ab}^d} - X_{h_{3a}^d}) \xi_{11}^{dL} \right]. \quad (\text{D.24})$$

For simplicity we restrict in the following to models without quark flavor violating, meaning either $\xi_{11} = 0$ or $\xi_{11} = 1$, which we take for the u - and d -sector uniformly. Couplings to nucleons are suppressed for $1 = C_u + C_d$, which implies for $\xi_{11} = 0$ models

$$X_{h_{ab}^u} + X_{h_{33}^u} - X_{h_{ab}^d} - X_{h_{33}^d} = 0, \quad (\xi_{11}^{uL} = \xi_{11}^{uR} = \xi_{11}^{dL} = \xi_{11}^{dR} = 0) \quad (\text{D.25})$$

and for $\xi_{11} = 1$ models

$$X_{h_{ab}^u} - X_{h_{ab}^d} = 0, \quad (\xi_{11}^{uL} = \xi_{11}^{uR} = \xi_{11}^{dL} = \xi_{11}^{dR} = 1). \quad (\text{D.26})$$

The condition for $\xi_{11} = 0$ can again only be satisfied if Higgses are pairwise identified. Since we also want $2N = 2X_{h_{ab}^u} + X_{h_{33}^u} - 2X_{h_{ab}^d} - X_{h_{33}^d}$ to be non-zero for the QCD axion, we finally arrive at the following necessary conditions for nucleophobia in models with $n \leq 3$:

$$X_{h_{ab}^u} = X_{h_{33}^d} \neq X_{h_{33}^u} = X_{h_{ab}^d}, \quad (\xi_{11}^{uL} = \xi_{11}^{uR} = \xi_{11}^{dL} = \xi_{11}^{dR} = 0) \quad (\text{D.27})$$

$$X_{h_{ab}^u} = X_{h_{ab}^d} \wedge X_{h_{33}^u} \neq X_{h_{33}^d}, \quad (\xi_{11}^{uL} = \xi_{11}^{uR} = \xi_{11}^{dL} = \xi_{11}^{dR} = 1), \quad (\text{D.28})$$

so that the contribution to the color anomaly effectively comes only from a single family, $2N = X_{h_{ab}^u} - X_{h_{ab}^d}$ for $\xi_{11} = 0$ and $2N = X_{h_{33}^u} - X_{h_{33}^d}$ for $\xi_{11} = 1$ (cf. Ref. [28]).

Comparing to the possible 3HDMs in Eq. (D.4), we see that for $\xi_{11} = 0$ only two structures allow for nucleophobia

$$\begin{aligned} \text{Q2:} \quad & y_u \sim \begin{pmatrix} h_a h_a \\ h_b h_b \end{pmatrix}, \quad y_d \sim \begin{pmatrix} h_b h_b \\ h_a h_a \end{pmatrix}, \\ \text{Q3:} \quad & y_u \sim \begin{pmatrix} h_a h_b \\ h_a h_b \end{pmatrix}, \quad y_d \sim \begin{pmatrix} h_b h_a \\ h_b h_a \end{pmatrix}, \end{aligned} \quad (\text{D.29})$$

with $a \neq b$, while for $\xi_{11} = 1$ there are also only two structures

$$\text{Q1:} \quad y_u \sim \begin{pmatrix} h_a h_a \\ h_a h_a \end{pmatrix}, \quad y_d \sim \begin{pmatrix} h_a h_b \\ h_a h_b \end{pmatrix},$$

Model	E_Q/N	$C_{u_i u_i}^A$	$C_{d_i d_i}^A$	$C_{u_i \neq u_j}^{V,A}$	$C_{d_i \neq d_j}^{V,A}$
Q1	$2/3 + 6c_\beta^2$	c_β^2	$\xi_{ii}^{d_R} - c_\beta^2$	0	$\xi_{ij}^{d_R}$
Q2	$-4/3 + 6c_\beta^2$	$c_\beta^2 - \xi_{ii}^{u_L}$	$-\xi_{ii}^{d_L} + s_\beta^2$	$\pm \xi_{ij}^{u_L}$	$\pm \xi_{ij}^{d_L}$
Q3	$-4/3 + 6c_\beta^2$	$c_\beta^2 - \xi_{ii}^{u_R}$	$-\xi_{ii}^{d_R} + s_\beta^2$	$-\xi_{ij}^{u_R}$	$-\xi_{ij}^{d_R}$
Q4	$-10/3 + 6c_\beta^2$	$-s_\beta^2 + \xi_{ii}^{u_R}$	s_β^2	$\xi_{ij}^{u_R}$	0

Table D2. Axion couplings in the four nucleophobic 2HDMs Q1-Q4, as a function of the flavor parameters ξ_{ij}^{qP} and the vacuum angle $c_\beta \equiv \cos \beta, s_\beta \equiv \sin \beta$. Here E_Q denotes the contribution of the quark sector to the electromagnetic anomaly coefficient E , to be added to the contribution E_L from the charged lepton sector. In all models the domain wall number is trivial, $2N = 1$. Nucleophobia is achieved for $C_u \approx 2/3, C_d \approx 1/3$.

$$\text{Q4: } y_u \sim \begin{pmatrix} h_c h_a \\ h_c h_b \end{pmatrix}, \quad y_d \sim \begin{pmatrix} h_c h_b \\ h_c h_a \end{pmatrix}, \quad (\text{D.30})$$

where $a \neq b$ and $c \neq a$ (otherwise Q4 = Q1). The notation is chosen such that in all models

$$2N = X_a - X_b, \quad C_u = \frac{X_a}{X_a - X_b}, \quad C_d = \frac{-X_b}{X_a - X_b}. \quad (\text{D.31})$$

This makes manifest that indeed $C_u + C_d = 1$, while the other condition for nucleophobia, $C_u - C_d = \frac{1}{3}$, requires for all models

$$\frac{1}{3} = \frac{X_a + X_b}{X_a - X_b}. \quad (\text{D.32})$$

For 2HDMs, without loss of generality $h_a = h_1$ and $h_b = h_c = h_0$, so that nucleophobia fixes the value of X_0 as

$$X_0 = -X_\phi A_1 \frac{v_1^2}{v^2} \stackrel{!}{=} -\frac{1}{3} A_1 X_\phi, \quad (\text{D.33})$$

with $v_1 \equiv s_\beta v, v_0 \equiv c_\beta v$, and thus nucleophobia is achieved for $s_\beta^2 \approx 1/3$. Note that the numerical value of A_1 is unphysical as it is equivalent to re-defining the PQ charge normalization. Choosing e.g. $A_1 = 1$ (corresponding to the operator $h_1^\dagger h_2 \phi$) and $X_\phi = 1$, one obtains $X_1 = c_\beta^2$ and $X_0 = -s_\beta^2$, and we recover the four nucleophobic models proposed in Ref. [28], although we follow the notation in Ref. [31]. The resulting predictions are summarized in Table D2.

In 3HDMs one has the possibility to enforce nucleophobia by making $X_0 \ll 1$ (instead of $X_0 \approx -1/3$), so that fermion couplings can be made small by coupling them to h_0 . This is because one can choose $h_a = h_1, h_b = h_2$ with $A_1 = 2, A_2 = -1$ (corresponding to the operators $h_1^\dagger h_0 \phi^2, h_2^\dagger h_0 \phi^\dagger$)

$$\frac{X_a + X_b}{X_a - X_b} = \frac{2X_0/X_\phi + A_1 + A_2}{A_1 - A_2} = \frac{1}{3} + \frac{2}{3} \frac{X_0}{X_\phi}. \quad (\text{D.34})$$

With

$$\frac{X_0}{X_\phi} = -\sum_i A_i \frac{v_i^2}{v^2} = \frac{v_2^2}{v^2} - 2 \frac{v_1^2}{v^2}. \quad (\text{D.35})$$

Model	E_Q/N	$C_{u_i u_i}^A$	$C_{d_i d_i}^A$	$C_{u_i \neq u_j}^{V,A}$	$C_{d_i \neq d_j}^{V,A}$
Q1	$14/3 + 2X_0$	$2/3 + X_0/3$	$-2/3 - X_0/3 + \xi_{ii}^{dR}$	0	ξ_{ij}^{dR}
Q2	$8/3 + 2X_0$	$2/3 + X_0/3 - \xi_{ii}^{uL}$	$1/3 - X_0/3 - \xi_{ii}^{dL}$	$\pm \xi_{ij}^{uL}$	$\pm \xi_{ij}^{dL}$
Q3	$8/3 + 2X_0$	$2/3 + X_0/3 - \xi_{ii}^{uR}$	$1/3 - X_0/3 + \xi_{ii}^{dR}$	$-\xi_{ij}^{uR}$	$-\xi_{ij}^{dR}$
Q4	$2/3 + 2X_0$	$-1/3 + X_0/3 + \xi_{ii}^{uR}$	$1/3 - X_0/3$	ξ_{ij}^{uR}	0
Q5	$2 + 2X_0$	$X_0/3 + 2/3 \xi_{ii}^{uR}$	$-X_0/3 + 1/3 \xi_{ii}^{dR}$	$2/3 \xi_{ij}^{uR}$	$1/3 \xi_{ij}^{dR}$

Table D3. Axion couplings in the five potentially nucleophobic 3HDM models Q1-Q5, as a function of the parameters ξ_{ij}^{qP} and X_0 . Here E_Q denotes the contribution of the quark sector to the electromagnetic anomaly coefficient E , to be added to the contribution from the charged lepton sector. In all models the domain wall number is $2N = 3$ and $X_0 \ll 1$. Nucleophobia is achieved for $C_u \approx 2/3, C_d \approx 1/3$.

and parametrizing the vevs as $v_0 = s_2 v, v_1 = c_1 c_2 v, v_2 = s_1 c_2 v$, one can choose vacuum angles such that $X_0/X_\phi = (1 - 3c_1^2)c_2^2 \ll 1$. How small X_0 can be only depends on constraints from perturbativity of Yukawa couplings. In models Q1-Q4 the strongest bounds come from SM top and bottom Yukawas, which are given by $y_t = y_t^{3\text{HDM}} c_1 c_2, y_b = y_b^{3\text{HDM}} s_1 c_2$, where $y_{b,t}^{3\text{HDM}}$ denote the couplings in the 3HDM, which neglecting running effects are bounded by $y_{b,t}^{3\text{HDM}} < \sqrt{16\pi/3} \approx 4.1$. For more details and the resulting constraints on nucleophobia see Ref. [30]. The constraints from perturbativity are relaxed in model Q5, which is obtained from the Q4 structure in Eq. (D.30) by choosing $h_c = h_0$ (while the 3HDM model Q4 is obtained from setting $h_c = h_b = h_2$). This is because only y_u and y_d are proportional to c_2 , while all other Yukawas are controlled by s_2 , so that c_2 can be chosen much smaller than in Q1-Q4 without being in conflict with perturbative unitarity. The resulting predictions for all models are summarized in Table D3, upon choosing $X_\phi = 1$.

D.5 Lepton Yukawa Sector

The general charged lepton Yukawa Lagrangian is given by

$$\mathcal{L} = y_{33}^e \bar{\ell}_{L3} e_{R3} \tilde{h}_{33}^e + y_{3a}^e \bar{\ell}_{L3} e_{Ra} \tilde{h}_{3a}^e + y_{a3}^e \bar{\ell}_{La} e_{R3} \tilde{h}_{a3}^e + y_{ab}^e \bar{\ell}_{La} e_{Rb} \tilde{h}_{ab}^e + \text{h.c.}, \quad (\text{D.36})$$

in the same notation as Eq. (D.1). We begin by restricting to a **2+1** flavor structure, denoting general Higgs couplings as

$$y_e \sim \begin{pmatrix} h_{ab}^e h_{a3}^e \\ h_{3a}^e h_{33}^e \end{pmatrix}, \quad (\text{D.37})$$

which fixes charged lepton charges in terms of Higgs charges as

$$X_{\ell_a} = X_{h_{33}^e} - X_{h_{a3}^e} + X_{\ell_3}, \quad X_{e_a} = X_{h_{3a}^e} + X_{\ell_3}, \quad X_{e_3} = X_{h_{33}^e} + X_{\ell_3}, \quad (\text{D.38})$$

and gives a single consistency condition

$$X_{h_{a3}^e} - X_{h_{33}^e} = X_{h_{ab}^e} - X_{h_{3a}^e}. \quad (\text{D.39})$$

Model	E_L/N	$C_{e_i e_i}^A$	$C_{e_i \neq e_j}^{V,A}$
E1	$2 - 6c_\beta^2$	$-c_\beta^2 + \xi_{ii}^{eL}$	$\mp \xi_{ij}^{eL}$
E2	$4 - 6c_\beta^2$	$s_\beta^2 - \xi_{ii}^{eL}$	$\pm \xi_{ij}^{eL}$

Table D4. Axion couplings in the two potentially electrophobic 2HDM models EL1 and EL2, as a function of the parameters ξ_{ij}^{eL} and $c_\beta \equiv \cos \beta, s_\beta \equiv \sin \beta$. Predictions for ER1 and ER2 are identical, upon $\xi_{ij}^{eL} \rightarrow \xi_{ij}^{eR}$ and in the last column $\mp \xi_{ij}^{eL} \rightarrow \xi_{ij}^{eR}, \pm \xi_{ij}^{eL} \rightarrow -\xi_{ij}^{eR}$. Here E_L denotes the contribution of the charged lepton sector to the electromagnetic anomaly coefficient E , to be added to the contribution from the quark sector. Electrophobia is achieved for $\xi_{11}^{eL} \approx c_\beta^2$ (E1) or $\xi_{11}^{eL} \approx s_\beta^2$ (E2) .

The contribution to the electromagnetic anomaly coefficient E_L is given by

$$E_L = -2X_{h_{ab}^e} - X_{h_{33}^e}, \quad (\text{D.40})$$

and axion couplings to charged leptons in the mass basis read

$$\begin{aligned} C_{ij}^{eL} &= (X_{h_{a3}^e} - X_{h_{33}^e} - X_{\ell_3}) \delta_{ij} - (X_{h_{a3}^e} - X_{h_{33}^e}) \xi_{ij}^{eL}, \\ C_{ij}^{eR} &= (-X_{h_{3a}^e} - X_{\ell_3}) \delta_{ij} + (X_{h_{3a}^e} - X_{h_{33}^e}) \xi_{ij}^{eR}. \end{aligned} \quad (\text{D.41})$$

Restricting to at most 3HDMs, again the consistency condition can only be pairwise satisfied, giving 2 possible structures, which are universal LH or RH charged lepton charges

$$y_e \sim \begin{pmatrix} h_d h_e \\ h_d h_e \end{pmatrix} \quad [ER] \quad \text{or} \quad y_e \sim \begin{pmatrix} h_d h_d \\ h_e h_e \end{pmatrix} \quad [EL] \quad (\text{D.42})$$

We are interested in suppressed electron couplings, which read

$$C_e \equiv C_e^A = \frac{1}{2N} \left(-X_d \delta_{ij} + (X_d - X_e) \begin{cases} \xi_{11}^{eR} & ER \\ \xi_{11}^{eL} & EL \end{cases} \right) \quad (\text{D.43})$$

In 2HDM, where both Higgs charges are large, the only way to suppress C_e is by tuning ξ_{11} . There are 2 possibilities for identifying h_d and h_e with h_0 and h_1 , giving

$$\begin{aligned} \text{E1 :} \quad y_e &\sim \begin{pmatrix} h_1 h_1 \\ h_0 h_0 \end{pmatrix}, \\ \text{E2 :} \quad y_e &\sim \begin{pmatrix} h_0 h_0 \\ h_1 h_1 \end{pmatrix}. \end{aligned} \quad (\text{D.44})$$

where we restricted to EL for simplicity, which gives identical predictions for axion couplings as ER, upon replacing $\xi_{ij}^{eL} \leftrightarrow \xi_{ij}^{eR}$. One finally obtains for 2HDMs the predictions in Table D4. Note that these models cannot be simultaneously electro- and muon- phobic if the conditions for nucleophobia and suppressed LFV couplings in the μ - e sector are imposed.

Model	E_L/N	$C_{e_i e_i}^A$	$C_{e_i \neq e_j}^{V,A}$
E1	$-4/3 - 2X_0$	$-X_0/3 - 2/3\xi_{ii}^{eL}$	$\pm 2/3\xi_{ij}^{eL}$
E2	$2/3 - 2X_0$	$-X_0/3 + 1/3\xi_{ii}^{eL}$	$\mp 1/3\xi_{ij}^{eL}$
E3	$-2X_0$	$-X_0/3$	0
E4	$-8/3 - 2X_0$	$-2/3 - X_0/3 + 2/3\xi_{ii}^{eL}$	$\mp 2/3\xi_{ij}^{eL}$
E5	$4/3 - 2X_0$	$1/3 - X_0/3 - 1/3\xi_{ii}^{eL}$	$\pm 1/3\xi_{ij}^{eL}$
E6	$-2/3 - 2X_0$	$-X_0/3 - \delta_{i3}/3$	$\pm\sqrt{2}/3 (\delta_{i2}\delta_{j3} + \delta_{i3}\delta_{j2})$

Table D5. Axion couplings in the six potentially electrophobic 3HDM models EL1-EL6, as a function of the parameters ξ_{ij}^{eL} and X_0 . Predictions for ER1-ER6 are identical, upon $\xi_{ij}^{eL} \rightarrow \xi_{ij}^{eR}$ and in the last column $\mp\xi_{ij}^{eL} \rightarrow \xi_{ij}^{eR}$, $\pm\xi_{ij}^{eL} \rightarrow -\xi_{ij}^{eR}$ and $\pm\sqrt{2}/3 \rightarrow -\sqrt{2}/3$ for ER6. Here E_L denotes the contribution of the charged lepton sector to the electromagnetic anomaly coefficient E , to be added to the contribution from the quark sector. One can check that $E_L/N = 2\sum_i C_{e_i e_i}^A$. Electrophobia is achieved for $X_0 \ll 1$ in E3 and additionally $\xi_{11}^{eL} \approx 0$ (E1,E2) or $\xi_{11}^{eL} \approx 1$ (E4,E5). The model E6 is special as all three leptons carry different PQ charges.

In 3HDMs, one can suppress the electron coupling simply by choosing $h_d = h_0$ ($\xi_{11} = 0$) or $h_e = h_0$ ($\xi_{11} = 1$), since X_0 has small PQ charge. Then there are in total 5 distinct choices (upon $L \leftrightarrow R$)

$$\begin{aligned}
\text{E1 : } \quad y_e &\sim \begin{pmatrix} h_0 h_0 \\ h_1 h_1 \end{pmatrix}, \\
\text{E2 : } \quad y_e &\sim \begin{pmatrix} h_0 h_0 \\ h_2 h_2 \end{pmatrix}, \\
\text{E3 : } \quad y_e &\sim \begin{pmatrix} h_0 h_0 \\ h_0 h_0 \end{pmatrix}, \\
\text{E4 : } \quad y_e &\sim \begin{pmatrix} h_1 h_1 \\ h_0 h_0 \end{pmatrix}, \\
\text{E5 : } \quad y_e &\sim \begin{pmatrix} h_2 h_2 \\ h_0 h_0 \end{pmatrix}.
\end{aligned} \tag{D.45}$$

They give rise to the models in Table D5. Note that E1 and E2 can be simultaneously electro- and muonphobic in the absence of lepton flavor violation ($\xi_{33} = 1$), while in E3 there is no LFV and all lepton couplings are small. Interestingly, for the 3HDM there are three combinations that are also photo-phobic, since they have $E/N = 2$, namely Q1E4, Q4E5, and Q5E3. In particular in model Q5E3 also all lepton couplings are small, so that there are sizable couplings only to first generation quarks, and couplings to nucleons and pions are also suppressed. This avoids essentially all phenomenological constraints, apart from mild SN1987A constraints from nucleon couplings. As discussed above, this also implies that constraints on vacuum angles from perturbative unitarity are very mild, thus allowing to achieve $X_0 \ll 1$ through $c_2 \ll 1$.

Finally we relax the assumption of a **2+1** flavor structure and consider the possibility

that in the charged lepton sector each lepton carries different PQ charge. We however still restrict to flavor universal charges for either LH or RH leptons, needed to satisfy the consistency constraints. Thus we consider two scenarios:

$$y_e \sim \begin{pmatrix} h_d h_e h_f \\ h_d h_e h_f \\ h_d h_e h_f \end{pmatrix} [ER] \quad \text{or} \quad y_e \sim \begin{pmatrix} h_d h_d h_d \\ h_e h_e h_e \\ h_f h_f h_f \end{pmatrix} [EL] \quad (\text{D.46})$$

This gives only models different than those discussed previously, if all three Higgses are different. Therefore the contribution E_L is fixed, and given by

$$E_L = -X_d - X_e - X_f = -(3X_0 + A_1 + A_2) = -3X_0 - 1, \quad (\text{D.47})$$

and

$$E_L/N = -\frac{2}{3}(3X_0 + 1) = -2X_0 - 2/3. \quad (\text{D.48})$$

Combining this model with Q2 or Q3 therefore gives a model with suppressed photon couplings. In addition we can simultaneously suppress electron and muon couplings. The charged lepton couplings read

$$(C_e^A)_{ij} = -\frac{1}{2N}(V_{EP}^*)_{ki}(V_{EP})_{kj}X_k, \quad (\text{D.49})$$

where $P = L/R$ for EL/ER and $X_k = \{X_d, X_e, X_f\}$. We now want to get suppression of the C_e, C_μ and $C_{e\mu}$ in order to avoid stringent constraints from WDs, SN1987A and LFV searches. This can indeed be achieved for choosing $h_d = h_0, h_e = h_1, h_f = h_2$, so

$$\text{E6 : } y_e \sim \begin{pmatrix} h_0 h_0 h_0 \\ h_1 h_1 h_1 \\ h_2 h_2 h_2 \end{pmatrix} \quad (\text{D.50})$$

for the LH model, the RH model is analogous. This gives

$$(C_e^A)_{ij} = -\frac{1}{3}[X_0\delta_{ij} - (V_{EL}^*)_{3i}(V_{EL})_{3j} + 2(V_{EL}^*)_{2i}(V_{EL})_{2j}]. \quad (\text{D.51})$$

Now choosing V_{EL} to be just a rotation in the 2-3 sector,

$$V_{EL} = \begin{pmatrix} 1 & & \\ & c_e & s_e \\ & -s_e & c_e \end{pmatrix}, \quad (\text{D.52})$$

with $s_e = \sqrt{2/3}, c_e = \sqrt{1/3}$, one finds

$$(C_e^A)_{ij} = -\frac{1}{3}X_0\delta_{ij} - \frac{1}{3} \begin{pmatrix} 0 & 0 & 0 \\ 0 & 0 & \sqrt{2} \\ 0 & \sqrt{2} & 1 \end{pmatrix}, \quad (\text{D.53})$$

so that diagonal and off-diagonal couplings in the E6 model read

$$(C_e^A)_{ii} = -\frac{1}{3}X_0 - \frac{1}{3}\delta_{i3}, \quad (C_e^{V,A})_{i \neq j} = \pm \frac{\sqrt{2}}{3}(\delta_{i2}\delta_{j3} + \delta_{i3}\delta_{j2}), \quad (\text{D.54})$$

and for $X_0 \ll 1$ only C_τ and $C_{\tau\mu}$ are non-vanishing.

References

- [1] R. D. Peccei and H. R. Quinn, *CP Conservation in the Presence of Instantons*, *Phys. Rev. Lett.* **38** (1977) 1440–1443.
- [2] R. D. Peccei and H. R. Quinn, *Constraints Imposed by CP Conservation in the Presence of Instantons*, *Phys. Rev. D* **16** (1977) 1791–1797.
- [3] S. Weinberg, *A New Light Boson?*, *Phys. Rev. Lett.* **40** (1978) 223–226.
- [4] F. Wilczek, *Problem of Strong P and T Invariance in the Presence of Instantons*, *Phys. Rev. Lett.* **40** (1978) 279–282.
- [5] L. Di Luzio, M. Giannotti, E. Nardi, and L. Visinelli, *The landscape of QCD axion models*, *Phys. Rept.* **870** (2020) 1–117, [[arXiv:2003.01100](#)].
- [6] J. Preskill, M. B. Wise, and F. Wilczek, *Cosmology of the Invisible Axion*, *Phys. Lett.* **B120** (1983) 127–132.
- [7] L. F. Abbott and P. Sikivie, *A Cosmological Bound on the Invisible Axion*, *Phys. Lett.* **B120** (1983) 133–136.
- [8] M. Dine and W. Fischler, *The Not So Harmless Axion*, *Phys. Lett.* **B120** (1983) 137–141.
- [9] **Planck** Collaboration, N. Aghanim et al., *Planck 2018 results. VI. Cosmological parameters*, *Astron. Astrophys.* **641** (2020) A6, [[arXiv:1807.06209](#)]. [Erratum: *Astron. Astrophys.* 652, C4 (2021)].
- [10] **Simons Observatory** Collaboration, P. Ade et al., *The Simons Observatory: Science goals and forecasts*, *JCAP* **02** (2019) 056, [[arXiv:1808.07445](#)].
- [11] **CMB-S4** Collaboration, K. N. Abazajian et al., *CMB-S4 Science Book, First Edition*, [[arXiv:1610.02743](#)].
- [12] L. J. Hall, K. Jedamzik, J. March-Russell, and S. M. West, *Freeze-In Production of FIMP Dark Matter*, *JHEP* **03** (2010) 080, [[arXiv:0911.1120](#)].
- [13] L. Caloni, M. Gerbino, M. Lattanzi, and L. Visinelli, *Novel cosmological bounds on thermally-produced axion-like particles*, *JCAP* **09** (2022) 021, [[arXiv:2205.01637](#)].
- [14] J. E. Kim, *Weak Interaction Singlet and Strong CP Invariance*, *Phys. Rev. Lett.* **43** (1979) 103.
- [15] M. A. Shifman, A. I. Vainshtein, and V. I. Zakharov, *Can Confinement Ensure Natural CP Invariance of Strong Interactions?*, *Nucl. Phys. B* **166** (1980) 493–506.
- [16] A. Notari, F. Rompineve, and G. Villadoro, *Improved Hot Dark Matter Bound on the QCD Axion*, *Phys. Rev. Lett.* **131** (2023), no. 1 011004, [[arXiv:2211.03799](#)].
- [17] F. D’Eramo, F. Hajkarim, and S. Yun, *Thermal QCD Axions across Thresholds*, *JHEP* **10** (2021) 224, [[arXiv:2108.05371](#)].
- [18] F. Bianchini, G. G. di Cortona, and M. Valli, *The QCD Axion: Some Like It Hot*, [[arXiv:2310.08169](#)].
- [19] M. Buschmann, C. Dessert, J. W. Foster, A. J. Long, and B. R. Safdi, *Upper Limit on the QCD Axion Mass from Isolated Neutron Star Cooling*, *Phys. Rev. Lett.* **128** (2022), no. 9 091102, [[arXiv:2111.09892](#)].

- [20] P. Carena, T. Fischer, M. Giannotti, G. Guo, G. Martínez-Pinedo, and A. Mirizzi, *Improved axion emissivity from a supernova via nucleon-nucleon bremsstrahlung*, *JCAP* **10** (2019), no. 10 016, [[arXiv:1906.11844](#)]. [Erratum: *JCAP* 05, E01 (2020)].
- [21] A. R. Zhitnitsky, *On Possible Suppression of the Axion Hadron Interactions. (In Russian)*, *Sov. J. Nucl. Phys.* **31** (1980) 260.
- [22] M. Dine, W. Fischler, and M. Srednicki, *A Simple Solution to the Strong CP Problem with a Harmless Axion*, *Phys. Lett. B* **104** (1981) 199–202.
- [23] R. Z. Ferreira and A. Notari, *Observable Windows for the QCD Axion Through the Number of Relativistic Species*, *Phys. Rev. Lett.* **120** (2018), no. 19 191301, [[arXiv:1801.06090](#)].
- [24] F. Arias-Aragón, F. D’Eramo, R. Z. Ferreira, L. Merlo, and A. Notari, *Production of Thermal Axions across the ElectroWeak Phase Transition*, *JCAP* **03** (2021) 090, [[arXiv:2012.04736](#)].
- [25] R. Z. Ferreira, A. Notari, and F. Rompineve, *Dine-Fischler-Srednicki-Zhitnitsky axion in the CMB*, *Phys. Rev. D* **103** (2021), no. 6 063524, [[arXiv:2012.06566](#)].
- [26] F. D’Eramo, E. Di Valentino, W. Giarè, F. Hajkarim, A. Melchiorri, O. Mena, F. Renzi, and S. Yun, *Cosmological bound on the QCD axion mass, redux*, *JCAP* **09** (2022) 022, [[arXiv:2205.07849](#)].
- [27] M. M. Miller Bertolami, B. E. Melendez, L. G. Althaus, and J. Isern, *Revisiting the axion bounds from the Galactic white dwarf luminosity function*, *JCAP* **10** (2014) 069, [[arXiv:1406.7712](#)].
- [28] L. Di Luzio, F. Mescia, E. Nardi, P. Panci, and R. Ziegler, *Astrophobic Axions*, *Phys. Rev. Lett.* **120** (2018), no. 26 261803, [[arXiv:1712.04940](#)].
- [29] F. Björkeroth, L. Di Luzio, F. Mescia, and E. Nardi, *$U(1)$ flavour symmetries as Peccei-Quinn symmetries*, *JHEP* **02** (2019) 133, [[arXiv:1811.09637](#)].
- [30] F. Björkeroth, L. Di Luzio, F. Mescia, E. Nardi, P. Panci, and R. Ziegler, *Axion-electron decoupling in nucleophobic axion models*, *Phys. Rev. D* **101** (2020), no. 3 035027, [[arXiv:1907.06575](#)].
- [31] M. Badziak, G. Grilli di Cortona, M. Tabet, and R. Ziegler, *Flavor-violating Higgs decays and stellar cooling anomalies in axion models*, *JHEP* **10** (2021) 181, [[arXiv:2107.09708](#)].
- [32] L. Di Luzio, F. Mescia, E. Nardi, and S. Okawa, *Renormalization group effects in astrophobic axion models*, *Phys. Rev. D* **106** (2022), no. 5 055016, [[arXiv:2205.15326](#)].
- [33] M. Badziak and K. Harigaya, *Naturally astrophobic QCD axion*, *JHEP* **06** (2023) 014, [[arXiv:2301.09647](#)].
- [34] F. Takahashi and W. Yin, *Hadrophobic axion from a GUT*, *Phys. Rev. D* **109** (2024), no. 3 035024, [[arXiv:2301.10757](#)].
- [35] **IAXO** Collaboration, A. Abeln et al., *Conceptual design of BabyIAXO, the intermediate stage towards the International Axion Observatory*, *JHEP* **05** (2021) 137, [[arXiv:2010.12076](#)].
- [36] S. Roy, C. Blanco, C. Dessert, A. Prabhu, and T. Temim, *Sensitivity of JWST to eV-Scale Decaying Axion Dark Matter*, [[arXiv:2311.04987](#)].
- [37] S. Chang and K. Choi, *Hadronic axion window and the big bang nucleosynthesis*, *Phys. Lett. B* **316** (1993) 51–56, [[hep-ph/9306216](#)].

- [38] G. Lucente, L. Mastrototaro, P. Carena, L. Di Luzio, M. Giannotti, and A. Mirizzi, *Axion signatures from supernova explosions through the nucleon electric-dipole portal*, *Phys. Rev. D* **105** (2022), no. 12 123020, [[arXiv:2203.15812](#)].
- [39] M. Gorghetto and G. Villadoro, *Topological Susceptibility and QCD Axion Mass: QED and NNLO corrections*, *JHEP* **03** (2019) 033, [[arXiv:1812.01008](#)].
- [40] K. Choi, S. H. Im, C. B. Park, and S. Yun, *Minimal Flavor Violation with Axion-like Particles*, *JHEP* **11** (2017) 070, [[arXiv:1708.00021](#)].
- [41] M. Chala, G. Guedes, M. Ramos, and J. Santiago, *Running in the ALPs*, *Eur. Phys. J. C* **81** (2021), no. 2 181, [[arXiv:2012.09017](#)].
- [42] M. Bauer, M. Neubert, S. Renner, M. Schnubel, and A. Thamm, *The Low-Energy Effective Theory of Axions and ALPs*, *JHEP* **04** (2021) 063, [[arXiv:2012.12272](#)].
- [43] K. Choi, S. H. Im, H. J. Kim, and H. Seong, *Precision axion physics with running axion couplings*, *JHEP* **08** (2021) 058, [[arXiv:2106.05816](#)].
- [44] Z.-Y. Lu, M.-L. Du, F.-K. Guo, U.-G. Meißner, and T. Vonk, *QCD θ -vacuum energy and axion properties*, *JHEP* **05** (2020) 001, [[arXiv:2003.01625](#)].
- [45] G. Grilli di Cortona, E. Hardy, J. Pardo Vega, and G. Villadoro, *The QCD axion, precisely*, *JHEP* **01** (2016) 034, [[arXiv:1511.02867](#)].
- [46] R. Bollig, W. DeRocco, P. W. Graham, and H.-T. Janka, *Muons in Supernovae: Implications for the Axion-Muon Coupling*, *Phys. Rev. Lett.* **125** (2020), no. 5 051104, [[arXiv:2005.07141](#)]. [Erratum: *Phys.Rev.Lett.* 126, 189901 (2021)].
- [47] D. Croon, G. Elor, R. K. Leane, and S. D. McDermott, *Supernova Muons: New Constraints on Z' Bosons, Axions and ALPs*, *JHEP* **01** (2021) 107, [[arXiv:2006.13942](#)].
- [48] A. Caputo, G. Raffelt, and E. Vitagliano, *Muonic boson limits: Supernova redux*, *Phys. Rev. D* **105** (2022), no. 3 035022, [[arXiv:2109.03244](#)].
- [49] A. Ayala, I. Domínguez, M. Giannotti, A. Mirizzi, and O. Straniero, *Revisiting the bound on axion-photon coupling from Globular Clusters*, *Phys. Rev. Lett.* **113** (2014), no. 19 191302, [[arXiv:1406.6053](#)].
- [50] D. B. Kaplan, *Opening the Axion Window*, *Nucl. Phys. B* **260** (1985) 215–226.
- [51] A. Jodidio et al., *Search for Right-Handed Currents in Muon Decay*, *Phys. Rev. D* **34** (1986) 1967. [Erratum: *Phys.Rev.D* 37, 237 (1988)].
- [52] **TWIST** Collaboration, R. Bayes et al., *Search for two body muon decay signals*, *Phys. Rev. D* **91** (2015), no. 5 052020, [[arXiv:1409.0638](#)].
- [53] L. Calibbi, D. Redigolo, R. Ziegler, and J. Zupan, *Looking forward to lepton-flavor-violating ALPs*, *JHEP* **09** (2021) 173, [[arXiv:2006.04795](#)].
- [54] **Belle-II** Collaboration, I. Adachi et al., *Search for Lepton-Flavor-Violating τ Decays to a Lepton and an Invisible Boson at Belle II*, *Phys. Rev. Lett.* **130** (2023), no. 18 181803, [[arXiv:2212.03634](#)].
- [55] F. D’Eramo, R. Z. Ferreira, A. Notari, and J. L. Bernal, *Hot Axions and the H_0 tension*, *JCAP* **11** (2018) 014, [[arXiv:1808.07430](#)].
- [56] D. Green, Y. Guo, and B. Wallisch, *Cosmological implications of axion-matter couplings*, *JCAP* **02** (2022), no. 02 019, [[arXiv:2109.12088](#)].

- [57] F. D’Eramo and S. Yun, *Flavor violating axions in the early Universe*, *Phys. Rev. D* **105** (2022), no. 7 075002, [[arXiv:2111.12108](#)].
- [58] CAST Collaboration, V. Anastassopoulos et al., *New CAST Limit on the Axion-Photon Interaction*, *Nature Phys.* **13** (2017) 584–590, [[arXiv:1705.02290](#)].
- [59] M. S. Turner, *Cosmic and Local Mass Density of Invisible Axions*, *Phys. Rev. D* **33** (1986) 889–896.
- [60] D. H. Lyth, *Axions and inflation: Sitting in the vacuum*, *Phys. Rev. D* **45** (1992) 3394–3404.
- [61] T. Hiramatsu, M. Kawasaki, K. Saikawa, and T. Sekiguchi, *Axion cosmology with long-lived domain walls*, *JCAP* **01** (2013) 001, [[arXiv:1207.3166](#)].
- [62] M. Kawasaki, K. Saikawa, and T. Sekiguchi, *Axion dark matter from topological defects*, *Phys. Rev. D* **91** (2015), no. 6 065014, [[arXiv:1412.0789](#)].
- [63] R. T. Co, L. J. Hall, and K. Harigaya, *QCD Axion Dark Matter with a Small Decay Constant*, *Phys. Rev. Lett.* **120** (2018), no. 21 211602, [[arXiv:1711.10486](#)].
- [64] P. Baratella, A. Pomarol, and F. Rompineve, *The Supercooled Universe*, *JHEP* **03** (2019) 100, [[arXiv:1812.06996](#)].
- [65] R. T. Co, E. Gonzalez, and K. Harigaya, *Axion Misalignment Driven to the Hilltop*, *JHEP* **05** (2019) 163, [[arXiv:1812.11192](#)].
- [66] K. Harigaya and J. M. Leedom, *QCD Axion Dark Matter from a Late Time Phase Transition*, *JHEP* **06** (2020) 034, [[arXiv:1910.04163](#)].
- [67] R. T. Co, L. J. Hall, and K. Harigaya, *Axion Kinetic Misalignment Mechanism*, *Phys. Rev. Lett.* **124** (2020), no. 25 251802, [[arXiv:1910.14152](#)].
- [68] M. Redi and A. Tesi, *Meso-inflationary QCD axion*, *Phys. Rev. D* **107** (2023), no. 9 095032, [[arXiv:2211.06421](#)].
- [69] K. Harigaya and L.-T. Wang, *More axions from diluted domain walls*, [arXiv:2211.08289](#).
- [70] X. Niu, W. Xue, and F. Yang, *Gauged Global Strings*, [arXiv:2311.07639](#).
- [71] T. Bessho, Y. Ikeda, and W. Yin, *Indirect detection of eV dark matter via infrared spectroscopy*, *Phys. Rev. D* **106** (2022), no. 9 095025, [[arXiv:2208.05975](#)].
- [72] R. Janish and E. Pinetti, *Hunting Dark Matter Lines in the Infrared Background with the James Webb Space Telescope*, [arXiv:2310.15395](#).
- [73] W. Yin et al., *First Result for Dark Matter Search by WINERED*, [arXiv:2402.07976](#).
- [74] P. Graf and F. D. Steffen, *Thermal axion production in the primordial quark-gluon plasma*, *Phys. Rev. D* **83** (2011) 075011, [[arXiv:1008.4528](#)].
- [75] A. Salvio, A. Strumia, and W. Xue, *Thermal axion production*, *JCAP* **01** (2014) 011, [[arXiv:1310.6982](#)].
- [76] R. T. Co and K. Harigaya, *Axiogenesis*, *Phys. Rev. Lett.* **124** (2020), no. 11 111602, [[arXiv:1910.02080](#)].
- [77] S. Scherer, *Introduction to chiral perturbation theory*, *Adv. Nucl. Phys.* **27** (2003) 277, [[hep-ph/0210398](#)].
- [78] F. D’Eramo, N. Fernandez, and S. Profumo, *Dark Matter Freeze-in Production in Fast-Expanding Universes*, *JCAP* **02** (2018) 046, [[arXiv:1712.07453](#)].

- [79] S. Hannestad, A. Mirizzi, and G. Raffelt, *New cosmological mass limit on thermal relic axions*, *JCAP* **07** (2005) 002, [[hep-ph/0504059](#)].
- [80] S. Borsanyi, Z. Fodor, J. N. Guenther, R. Kara, S. D. Katz, P. Parotto, A. Pasztor, C. Ratti, and K. K. Szabo, *QCD Crossover at Finite Chemical Potential from Lattice Simulations*, *Phys. Rev. Lett.* **125** (2020), no. 5 052001, [[arXiv:2002.02821](#)].
- [81] L. Di Luzio, G. Martinelli, and G. Piazza, *Breakdown of chiral perturbation theory for the axion hot dark matter bound*, *Phys. Rev. Lett.* **126** (2021), no. 24 241801, [[arXiv:2101.10330](#)].
- [82] L. Di Luzio, J. Martin Camalich, G. Martinelli, J. A. Oller, and G. Piazza, *Axion-pion thermalization rate in unitarized NLO chiral perturbation theory*, *Phys. Rev. D* **108** (2023), no. 3 035025, [[arXiv:2211.05073](#)].
- [83] A. Alloul, N. D. Christensen, C. Degrande, C. Duhr, and B. Fuks, *FeynRules 2.0 - A complete toolbox for tree-level phenomenology*, *Comput. Phys. Commun.* **185** (2014) 2250–2300, [[arXiv:1310.1921](#)].
- [84] V. Shtabovenko, R. Mertig, and F. Orellana, *New Developments in FeynCalc 9.0*, *Comput. Phys. Commun.* **207** (2016) 432–444, [[arXiv:1601.01167](#)].
- [85] V. Shtabovenko, R. Mertig, and F. Orellana, *FeynCalc 9.3: New features and improvements*, *Comput. Phys. Commun.* **256** (2020) 107478, [[arXiv:2001.04407](#)].
- [86] A. Czarnecki, M. Kamionkowski, S. K. Lee, and K. Melnikov, *Charged Particle Decay at Finite Temperature*, *Phys. Rev. D* **85** (2012) 025018, [[arXiv:1110.2171](#)].
- [87] D. Cadamuro, S. Hannestad, G. Raffelt, and J. Redondo, *Cosmological bounds on sub-MeV mass axions*, *JCAP* **02** (2011) 003, [[arXiv:1011.3694](#)].
- [88] K. Saikawa and S. Shirai, *Primordial gravitational waves, precisely: The role of thermodynamics in the Standard Model*, *JCAP* **05** (2018) 035, [[arXiv:1803.01038](#)].
- [89] F. D’Eramo and A. Lenoci, *Lower mass bounds on FIMP dark matter produced via freeze-in*, *JCAP* **10** (2021) 045, [[arXiv:2012.01446](#)].
- [90] P. Panci, D. Redigolo, T. Schwetz, and R. Ziegler, *Axion dark matter from lepton flavor-violating decays*, *Phys. Lett. B* **841** (2023) 137919, [[arXiv:2209.03371](#)].